THE PORE SIZE DISTRIBUTION OF PORTLAND CEMENT PASTE

DECEMBER 1968
NO. 31

by

D N. WINSLOW

Joint Highway Research Project

PURDUE UNIVERSITY
LAFAYETTE INDIANA

Final Report

THE PORE SIZE DISTRIBUTION OF PORTLAND CEMENT PASTE

To: J. F. McLaughlin, Director
Joint Highway Research Project

February 14, 1969

Project: C-36-61E

From: H. L. Michael, Associate Director
Joint Highway Research Project

File: 5-14-5

The attached report "The Pore Size Distribution of Portland Cement Paste" is the Final Report on Phase I of the HPR Part II research project "Fundamental Studies in Portland Cement Concrete, Phase I". The report has been authored by Mr. D. N. Winslow, Graduate Assistant in Research on our staff, under the direction of Professor Sidney Diamond. Mr. Winslow also used the report for his MSCE thesis.

The report reviews theories of pore size distribution measurement and both theoretical and practical size limits are discussed. In this study mercury intrusion was used to measure pores of one size and capillary condensation was used for another size. Details of each technique and equipment together with results are given for cement paste samples.

The results of this Phase I also resulted in a proposal for PhaseII of this research. This proposed Phase II has already been submitted for review and action.

This report is submitted for the record and acceptance. It will also be forwarded to the BPR and the ISHC for their review, comment and acceptance.

Respectfully submitted,

Harold L. Michael

Harold L. Michael
Associate Director

HLM:rg

cc: F. L. Ashbaucher, W. L. Dolch, W. H. Goetz, W. L. Grecco, G. K. Hallock, M. E. Harr, R. H. Harrell, J. A. Havers, V. E. Harvey, G. A. Leonards, F. B. Mendenhall, R. D. Miles, C. F. Scholer, M. B. Scott, W. T. Spencer, H. R. J. Walsh, K. B. Woods, E. J. Yoder

Final Report- Phase I

THE PORE SIZE DISTRIBUTION OF PORTLAND CEMENT PASTE

by

D. N. Winslow
Graduate Assistant in Research

Prepared as Part of an Investigation

Conducted by

Joint Highway Research Project
Engineering Experiment Station
Purdue University

in cooperation with the

Indiana State Highway Commission

and the

U.S. Department of Transportation
Federal Highway Administration
Bureau of Public Roads

Purdue University
Lafayette, Indiana
December 18, 1968

ACKNOWLEDGMENTS

This writer wishes to express his sincere appreciation to his major professor, Dr. Sidney Diamond, for his guidance, help and understanding during the long course of this research and the writing of this report. Also, the advice of Dr. William L. Dolch was very helpful and greatly appreciated.

This writer must also express his appreciation to his father, Dr. Nathaniel M. Winslow, for his counsel and for the development and design of the major portion of the equipment used in this work.

Mr. Jerry Isenburg, Mr. Everett Sutton and the Dow Chemical Company should be thanked as they made available the use of, and pictures from, a scanning electron microscope. Many other people were of great assistance in the technical phases of this work.

This research was sponsored by the Indiana State Highway Department and the Bureau of Public Roads, U. S. Department of Transportation and was administered through the Joint Highway Research Project.

Finally, this author wants to thank his wife, Linda, for a great deal of patient understanding and self-sacrifice while this research was in progress.

TABLE OF CONTENTS

TABLE OF CONTENTS (cont'd.)

LIST OF TABLES

LIST OF FIGURES

Figure Page

ABSTRACT

Winslow, Douglas Nathaniel. M.S.C.E., Purdue University, January 1969. The Pore Size Distribution of Portland Cement Paste. Major Professor: Sidney Diamond.

A review of published pore size distribution curves for Portland cement paste is made with particular attention to the method of measurement and the range of pore diameters measured. Theories of pore size distribution measurement are examined and both theoretical and practical size limits are discussed. In this work mercury intrusion was used to measure pores with diameters between 1000 μ and 0.0085 μ and capillary condensation (using water vapor) was used between the pore diameter limits of 0.1000 μ and 0.0030 μ. Equipment and experimental details of the mercury intrusion technique discussed in detail include necessary modifications to a commercially available porosimeter, the design and use of a new macro-pore porosimeter and specific assessment of such factors as the difference between theoretical and effective mercury compressibility and heating due to compression. A direct measurement of the factor $(-4\gamma\cos\theta)$ for mercury on cement paste is described. Experimental detail and equipment used to measure the capillary condensation on cement paste are described. Particular attention is paid to the matter of sorption equilibrium and the various factors affecting equilibrium and rate of sorption are qualitatively assessed.

All cement paste samples were mixed in a vacuum, cast so as to avoid entrapping air bubbles and hydrated in saturated $Ca(OH)_2$ solution.

Details of mixing, placing, curing, and sampling are given. Density of solids calculations from bouyant weight in water provided an estimate of total pore volume for all samples.

Mercury intrusion is used to measure the pore size distributions of cement pastes of two water:cement ratios (0.4 and 0.6) at nine ages (1,2,3,5.7,28,60,267 and 320 days). The effects of drying technique (oven drying, "P" drying and "D" drying) and atmospheric carbonation on the measured pore size distributions are examined in detail. Particular attention is paid to the mercury intrusion equilibrium time as a function of pore diameter. Capillary condensation is applied to a mature (267 day old) cement paste of each water:cement ratio. The method of Roberts is applied for the data reduction using an adsorption isotherm with the special feature of outgassing the sample between steps. The necessary "t-curve" for water vapor is presented and its measurement (on crushed quartz) is described.

The mercury intrusion pore size distributions invariably display a characteristic pore diameter above which little pore volume is detected and immediately below which an appreciable fraction of the total measured pore volume is intruded. This "threshold" diameter decreased with increasing age and decreasing water:cement ratio. The volume intruded increased continuously from the threshold diameter to the lower measurement limit. From measurements of intrusion equilibrium times and photographs of intruded and fractured samples it is seen that the threshold diameter represents the largest pore size which is structurally continuous throughout the cement paste.

The water vapor pore size distribution curve for the 0.6 water:

cement ratio paste shows remarkable agreement with the mercury intrusion curves. The two distributions are coincident except for a small deviation in the diameter range 0.10 μ to 0.04 μ. The distributions of the 0.4 water:cement ratio paste exhibit a similar deviation and a second, larger deviation is observed in the diameter range 0.0250 μ to 0.0085 μ. In all cases the water vapor measures a greater pore volume than does the mercury and the deviations are presumed to be caused by restricted entryways into pores.

Data on water vapor and nitrogen B.E.T. surface areas and areas calculated from pore size distributions are presented.

INTRODUCTION

This investigation was undertaken to determine as completely as possible the pore size distribution of hardened Portland cement paste. In addition to measuring pore diameters over a wide range, the effects of water:cement ratio and degree of hydration (age) were investigated.

Portland cement is best defined by ASTM Standard C-150. In this research Type I cement was used. An analysis of the cement (Lab. No. 317) is to be found in Appendix A. When Portland cement and water are mixed a reaction begins. This reaction results in the stiffening and eventual hardening of the Portland cement mix into what is known as hardened Portland cement paste. Briefly, the composition of this hardened cement paste is the solid products of the reaction, any solid Portland cement which has not reacted, and voids or pores.

When an aggregate, i.e., some form of solid filler, is mixed along with the water and cement the resulting hardened body is either a mortar or a concrete. The difference between the two lies in the maximum size of aggregate present, mortars having a smaller maximum size. The hardened Portland cement paste which exists between the pieces of aggregate is essentially a "glue" which holds the pieces together. This glue is thought to have the same properties as pure hardened Portland cement paste except, of course, that the aggregate acts to break up the space continuity of the paste.

As mentioned, the paste is made up of solid particles and pores.

Some of the solid particles may be unreacted cement, and generally these have linear dimensions of several microns or larger. The reaction products of the water and cement are also particulate and dimensions on the order of one thousand Angstroms are appropriate to describe most of them. The pores may exist between the unreacted particles, between the reacted particles or between a reacted and unreacted particle. Further, bubbles of air trapped at the time of mixing may be present.

The total pore volume of a hardened Portland cement paste is then the sum of the volume of all these pores. The pore size distribution of cement paste is the manner in which the total volume of pores is mathematically distributed with respect to the diameter of the pores. Thus, a complete pore size distribution contains the same information as a total pore volume and additionally includes further information on the volume of the pores of various diameters which make up the total.

As Portland cement paste is the glue which holds Portland cement concrete together, its properties must be of considerable importance to the properties of the concrete as a whole. If it fails to hold the mass together the strength of the concrete will be reduced to that of a pile of aggregate. Since the paste surrounds the aggregate the flow of fluids through concrete will be controlled by the paste through which the fluid must pass.

Powers (15)* has shown that the ratio of the volume of the solid reaction products of the cement and water to the total volume of the pores in the paste markedly affects the strength of the paste. Powers (16) has also shown that the pore volume affects the permeability of cement paste and, since in a well compacted concrete this paste envelops

* Numbers in parentheses refer to references at the end of this thesis.

the aggregate, it must affect the permeability of the concrete.

However, a gross measurement of pore volume is not necessarily sufficient to correlate completely the porosity and the properties. For example, Portland cement concrete cannot be damaged by freezing and thawing unless some of the water in the pores freezes, but water in very small pores will not freeze at common outdoor temperatures. Furthermore, water flowing through large pores causes little trouble; however, if the diameter of the pore is small enough, forced flow of water will rupture the pore walls. In these two examples it is clearly the diameter of the pores and not merely the total pore volume that is of importance. Only a pore size distribution yields information about pore diameters.

A search of the literature has revealed several published determinations of pore size distributions. However, these are all incomplete in one or more of the following respects: range of diameters over which measurements were made; range of ages of samples tested, range of water: cement ratios of samples tested, and finally a lack of appreciation of the effect of assumptions and experimental techniques on the measured pore size distribution.

Edelman, Sominskii and Kopchikova (6) report pore size distributions for three water:cement ratios (0.28, 0.5, 0.7) at one age (28 days), and for one of these water:cement ratios (0.28) at three additional ages (1 day, 5 months and 1 year). The range of pore diameters measured is from about 200μ to about 0.012μ.

The Scientific Instruments Division of Carlo Erba (2) has reported pore size distribution curves at six ages (1,2,3,7,14 and 28 days) at unknown water:cement ratios. The range of measured pore diameters is 6μ to

0.02μ.

Both of the above investigations used a technique known as mercury intrusion. The present worker, having very thoroughly investigated this technique, believes that insufficient thought was given to the assumptions made in analyzing the data and to the techniques of sample preparation. The effects of both these factors, as well as the basic method of measurement, will be discussed later.

Mikhail, Copeland and Brunauer (11) show differential pore size distributions for two water:cement ratios (0.35 and 0.50) at one age (12 years) and one distribution for a water:cement ratio of 0.70 at an age of 2.5 years. In all cases the range of pore diameters is 0.03μ to 0.02μ.

Mikhail and Selim (12) report differential pore size distributions for a water:cement ratio of 0.35 at an age of 12 years and for a water:cement ratio of 0.70 at an age of 2.5 years. The range of diameters measured is 0.03μ to 0.002μ.

In the two above papers the method of capillary condensation was used to determine the pore size distribution. The authors of the first named paper employed nitrogen, and those of the second cyclohexane as the condensable vapor. Both of the above papers cover a rather narrow range, and by the authors' own admission, use a vapor which is incapable of reaching all the pores.

The present investigation was undertaken owing to the paucity of information on the pore size distribution as indicated above. The Portland cement described in Appendix A was used throughout. Two water:cement ratios were investigated: 0.4 and 0.6. These roughly correspond to the extremes generally encountered in practical concrete technology. Pastes

of both water:cement ratios hydrated for the following periods were studied: 1,2,3,5,7,28,60 and 320 days. In all cases pore size distributions were obtained over a range of diameters from 210μ to 0.0085μ. The larger limit of the range was initially 1000μ but as no cement paste was found to have any pores of such large diameters the limit was lowered to 210μ for experimental convenience. Additionally, one paste of each water:cement ratio at an age of 267 days was investigated over a pore diameter range of 210μ to 0.002μ.

There are two principle methods of determining a pore size distribution: mercury intrusion and capillary condensation. These have already been mentioned and will shortly be discussed in greater detail. Theoretically, either method is capable of measuring pores over a very wide range but practically both methods have fairly clearly defined regions of applicability. In this work mercury intrusion covered a range of diameters of 210μ to 0.0085μ and capillary condensation a range of 0.1μ to 0.002μ.

Mercury intrusion was used as the principle investigative tool. All of the first mentioned tests (the two water:cement ratios at eight ages) were conducted with this method. The last two mentioned tests (at an age of 267 days) were combinations of the two methods. Thus, the range of pore diameters was extended in the smaller region and an area of overlap between the two methods was obtained. In this region agreement between the two methods was hoped for in order to engender more confidence in the results.

THEORIES OF PORE SIZE MEASUREMENT

General Considerations

The two commonly used techniques of measuring pore size distributions, and those used herein, are capillary condensation and mercury intrusion. Both are founded on the phenomenon of surface tension or the surface free energy of a liquid. Both methods are applicable only to those pores which have some communication with the exterior of a porous body. Hence, data so obtained must always be viewed as the pore size distribution of those pores which are so interconnected as to be open to the exterior.

Both methods rely on the existence, in a pore, of a liquid which has the same properties as the bulk liquid. And, in particular, it is necessary to assume that the surface (meniscus) of the liquid in the pore behaves as does the surface of the liquid in the bulk state. The above constraint sets a small pore limit on the diameters measurable by either technique. As the diameter of a pore approaches several molecular diameters of the liquid in the pore, the meniscus of the liquid can no longer be thought of as being the same as it would be in a much larger pore. By way of example, both methods require that a contact angle exist between the liquid and the solid pore wall. Consider a pore of a diameter equal to the molecular diameter of the liquid. Here the entire concept of contact angle vanishes. Thus, it is seen that the small pore diameter limit of either technique is fixed by the molecular diameter of the liquid used,

and the smallest pore measurable must be some multiple of the molecular diameter. Unfortunately, there is no method presently available with which to determine exactly what this multiple should be. Brunauer (10) and Drake (5) have suggested that a meniscus in a pore whose diameter is about ten times the molecular diameter will behave as would a much larger meniscus.

There is no theoretical upper limit to the measurable pore diameter set by either method. However, practical experimental restrictions do impose upper limits. In the case of capillary condensation the problem is one of maintaining very high partial pressures of a vapor throughout a system. For example, to differentiate between a pore of a diameter of five microns and a pore of ten microns diameter would entail the maintenance of partial pressures on the order of 0.99995 and 0.99996 and, it would be essential to be able to differentiate one from the other. As a rule then, the upper limit for capillary condensation is in practice a diameter of about 0.1μ.

Mercury intrusion is limited by the difficulty of applying a very small pressure to a liquid without the head of the liquid itself supplying that pressure. It is necessary to block off the mouth of a pore to be measured with mercury and then to apply pressure. If the head of mercury can supply the pressure required the mercury will intrude the pore without benefit of any experimentally controllable pressuring and the measurement is lost. This sets the upper limit of the method at about a diameter of 1000μ. With special techniques this might be raised to several thousands of microns but this is about the limit.

Capillary Condensation

Considerations of the surface energy of a liquid lead to the result that the vapor pressure of a curved liquid surface is different than that of a flat liquid surface. A pore provides a location for a curved surface to form. As the radius of curvature of condensate in a pore decreases the pressure of vapor in equilibrium with this condensate decreases. Because of this vapor will condense in a sufficiently small pore at a partial pressure well below the saturation pressure normally required for condensation on a flat surface.

The fundamental expression of this phenomenon is the Kelvin equation (19):

$$d = \frac{-4 \gamma M \cos \theta}{RT \rho \ln P/P_o}$$

where:

d = diameter of the curved liquid surface

γ = surface energy of the liquid

M = molecular weight of the liquid

θ = contact angle of liquid and solid

R = gas constant

T = absolute temperature of liquid

ρ = density of liquid

P/P_o = partial pressure of vapor

With this equation and a vapor sorption isotherm it is possible to calculate a pore size distribution. When a condensable vapor is exposed to a porous solid three things may happen. The vapor may chemically interact with the solid. It may be physically sorbed onto the surface of the solid. And, in pores of certain sizes it may condense and fill the

pore. Only the latter two will be considered here.

Normally both sorption and condensation will occur at the same time, and a measured isotherm shows only the combined effect of the two. To obtain a pore size distribution it is necessary to separate the condensation from the sorption. This was accomplished as described later. The procedure involves relating the partial vapor pressure to the pore diameter, in which condensation is occurring and using the volume of vapor sorbed, with suitable corrections, as a measure of pore volume.

Mercury Instrusion

When a liquid forms a contact angle with a solid greater than 90°, it is said to be nonwetting. The relatively high surface tension of such a liquid opposes its entry into pores in the solid. This is the phenomenon of capillary depression. Pressure applied to the liquid will overcome this opposition and the nonwetting liquid will enter the pore. The pressure required to accomplish this is a function of the surface properties of the liquid and the solid and the geometry of the pore.

For the case of a cylindrical pore the functional relationship (22) is:

$$P = \frac{-4 \gamma \cos \theta}{d}$$

where: P = pressure required to overcome opposition to entry

d = diameter of pore being entered

γ = surface energy of liquid entering

θ = contact angle between liquid and pore wall

This equation is valid for any system in which the liquid and solid do not chemically interact. As a practical matter, however, mercury is the commonly used liquid. This is because it does not interact with many

solids under reasonable conditions; it forms a contact angle greater than 90° with many solids, and it has a low vapor pressure. This latter advantage is one of significant experimental convenience.

All pore size distributions measured in this work by the use of this phenomenon were done with mercury. Hence, the term mercury intrusion will be used in this writing. However, it sould be kept in mind that mercury is just a convenient liquid and not solely responsible for this phenomenon, and perhaps a better name for this would be "forced intrusion of a nonwetting liquid".

If the quantity ($-4\ \gamma \cos \theta$) is known then the simple inverse relation existing between the pressure causing intrusion and the diameter of the pore being intruded may be used for calculating diameters from known values of pressure. Most pore size distribution work using mercury intrusion uses handbook values for the surface energy and angle of contact. In this work a direct measurement of the quantity ($-4\ \gamma \cos \theta$) was made for the system being studied. A complete description of this measurement is to be found in Appendix B. With the result of this measurement the above equation was used to relate pressures measured during experiments and the diameter of pores being intruded. The volume of the pores being intruded was determined by measuring the volume of mercury which was forced into the sample.

APPARATUS, EXPERIMENTAL TECHNIQUES AND REDUCTION OF DATA

Cement Paste Mixing and Curing

Portland cement paste samples were needed for this research which were homogeneous and free from accidentally trapped air bubbles. Homogeneity was desired so that various pieces selected from the same mixing batch would yield similar pore size distributions. Trapped air voids were undesirable as they could cause arbitrary fluctuations in pore size distributions. Additionally, a standard and reproducible technique of mixing and casting was necessary to avoid fluctuations from this source.

The following technique has been found to satisfactorily meet these requirements. It was devised by Mullen (13) and Hanna (9) and, as they state, is the result of trial and error. The exact times and other particulars involved are merely those that were found to give satisfactory results.

Cement Paste Mixer

The basic mixing drum was a plastic cylinder about 30 cm long and 15 cm in diameter. One end was sealed permanently and the other end threaded to permit removal of the end plate. The removable end sealed to the unit by means of an O-ring. A stopcock was located in the fixed end to permit evacuation and to admit water. A collection of solid objects was placed in the mixing drum to promote mixing. These included six steel rods, about one centimeter in diameter and ten centimeters

long, and ten almost spherical flint balls, about two centimeters in diameter. The rods and balls were free to roll and tumble in the mixing drum. The cylinder was rotated on an electric paint roller during a portion of the mixing operation.

Mixing Cement Paste

Deionized water was degassed in a 1000 ml filter flask using an aspirator for 15 min. A 1000 g portion of Lab No. 317 Portland cement was placed into the thoroughly dry mixing chamber. The steel rods and flint balls were added and the removable end plate was screwed on. The mixing chamber was outgassed with an aspirator for 15 min. The degassed water was next poured into a graduated cylindrical separatory funnel. This was done carefully to avoid entrapping or dissolving gas in the water. The evacuated cylinder was closed with the stopcock and removed from the aspirator. The proper amount of water to yield the desired water:cement ratio was then drawn from the funnel into the mixer through the stopcock. This was done in such a way as to admit no air. The stopcock was closed again after the addition of the water.

The mixing chamber was then shaken by hand, for two minutes, in a motion not dissimilar to that used with a cocktail shaker. The mixer was next rolled on the electric roller for five minutes at 100 revolutions per minute. The mixer was then shaken for two minutes, rolled for five minutes, shaken for two minutes, rolled for five minutes, and finally shaken for two minutes.

The vacuum was released by opening the stopcock and the threaded cap removed. The paste was poured into clean, dry 12 ml polypropylene round bottom test tubes which were approximately 100 mm long and 15 mm in

diameter. A single mix was sufficient to fill 20 such tubes. Each tube was filled on a vibrating table in the following manner: the tube was filled one third full and then rodded 25 times with a small steel rod. This process was then repeated for the second and final thirds. The full tubes were left to vibrate for two minutes. Each tube was then closed with a rubber stopper which left essentially no free volume between the stopper and the paste. In an effort to reduce sedimentation the tubes were then manipulated as follows: they were placed stopper down and vibrated for 2 min, then were left still, in this position, for 20 min. They were next turned stopper up, vibrated for two minutes and left still for eight minutes. Then they were turned stopper down, vibrated for two minutes and left still for eight minutes. Finally the tubes were turned stopper up and vibrated for two minutes. This completed the mixing and placing operations.

Curing Cement Paste

For 24 hours following mixing and placement the tubes of cement were stored, stopper up, in a fog room. The atmosphere of the room was constantly saturated with water and the temperature was about 24°C.

After 24 hours the samples were removed from the tubes. This was done by taking advantage of the difference in thermal expansion of the tube and the cement paste. The tube was placed in a 65°C water bath for about one minute and then the cement paste cylinder was slid out. The cylinders were slid directly into a jar containing a saturated solution of $Ca(OH)_2$ and deionized water so that they would not lose moisture during the process of removal. The samples continued to hydrate in the jar until they attained the desired age for testing.

Cement Paste Sampling and Drying

Sampling Cement Paste

When a sample had reached the desired age for testing it was removed from the $Ca(OH)_2$ solution. The center one-third of the cylinder was cut out with a diamond saw and the two ends discarded. Density measurements of slices along the entire length of cylinder were made by this author and by S. J. Hanna (during his research) and, although some variation was found at the top and bottom, the central section was found to be very uniform. The center section was cut into three pieces about one centimeter in length. At least two cylinders of each age were sampled in this manner. Buoyant and saturated surface dry weights were obtained for each piece. To avoid accidental drying before these measurements could be made the samples were kept under water as much as possible during sampling and the cutting operation was done as rapidly as possible. The buoyant weight of each piece was measured by suspending the piece from an analytical balance into a beaker of water. Then each sample was rapidly dried with a moist towel. This removed essentially all of the loose surface water but not the water held in the pores. After this surface drying the sample was rapidly weighed on an analytical balance.

Techniques of Drying Cement Paste

After these operations the samples were dried. Four methods of drying were used including the commonly termed "D" and "P" drying methods, drying in an oven held at 105°C and a combination of air and oven drying.

The "D" drying (4) was carried out in a desiccator connected to a vacuum pump with a cold trap between the pump and the desiccator. The

cold trap was kept in a bath of trichloroethylene and dry ice (solid CO_2). Thus, all moisture leaving the samples was frozen in the trap and was held at the temperature of the dry ice, -78°C. This fixed the vapor pressure of the system at 0.5μHg.

"P" drying (14) was also carried out in a desiccator. A mixture of $Mg(ClO_4)_2 \cdot 2H_2O$ and $Mg(ClO_4)_2 \cdot 4H_2O$ was prepared by adding sufficient water to analytical reagent grade anhydrous $Mg(ClO_4)_2$ to insure that all of it would have at least the form $Mg(ClO_4)_2 \cdot 2H_2O$. Enough of this desiccant was prepared so that when all of the moisture in the samples had been transferred to the desiccant not all of the desiccant would be converted to the form $Mg(ClO_4)_2 \cdot 4H_2O$. Thus, the vapor pressure in the desiccator was fixed at eight microns Hg (14).

Oven drying was done by simply placing the samples in standard laboratory oven which was kept at 105°C.

The combination air and oven drying was begun by allowing the samples to dry to equilibrium with the atmosphere of the laboratory. The temperature of the laboratory was about 23°C and the relative humidity was about 35%. After this equilibration the samples were dried in the oven in the same manner as the oven dried samples.

During all types of drying the samples were weighed periodically on an analytical balance and the final equilibrium weight was recorded. In general, about three weeks were required to dry the samples by the "P", "D" or air/oven drying techniques while oven drying usually required one day.

Mercury Intrusion Porosimetry

Mercury Intrusion Apparatus

The basic mercury intrusion instrument* used in this investigation consists of a pressure chamber in which 15,000 psi can be generated, a motor driven means of creating this pressure, Bourdon tube gauges for reading the pressure and a means of sensing the intrusion of mercury.

The sample to be tested is housed in a sample holder which is much like a dilatometer and is called a penetrometer. This is illustrated in Figure 1 which shows a penetrometer disassembled, one assembled and containing a sample of cement paste and a penetrometer (containing a sample) filled with mercury. When filled with mercury, intrusion is measured (either visually or mechanically) by the change in position of the mercury meniscus in the capillary stem. When intrusion occurs this meniscus moves toward the bulb end of the penetrometer. Except where noted, this research was conducted with penetrometers having a sample bulb volume of about 6 ml, a precision bore capillary stem diameter of 1.3 mm and a total bore volume of 0.2 ml. Calibrations are scribed on the stem at intervals of 0.002 ml.

In the instrument, pressure is generated by an electrically driven hydraulic pump. The pressure is measured with two Bourden tube gauges, the capacities of which are 1000 psi and 15000 psi. The smallest increment on the 1000 psi gauge is 5 psi and on the 15000 psi gauge 100 psi. The manufacturer's stated accuracy for both gauges is ± 0.25% of their full scale reading for any pressure within their range. The 1000 psi gauge was tested over the range 0-100 psi and the error was found to be

* American Instrument Company Cat. No. 5-7121.

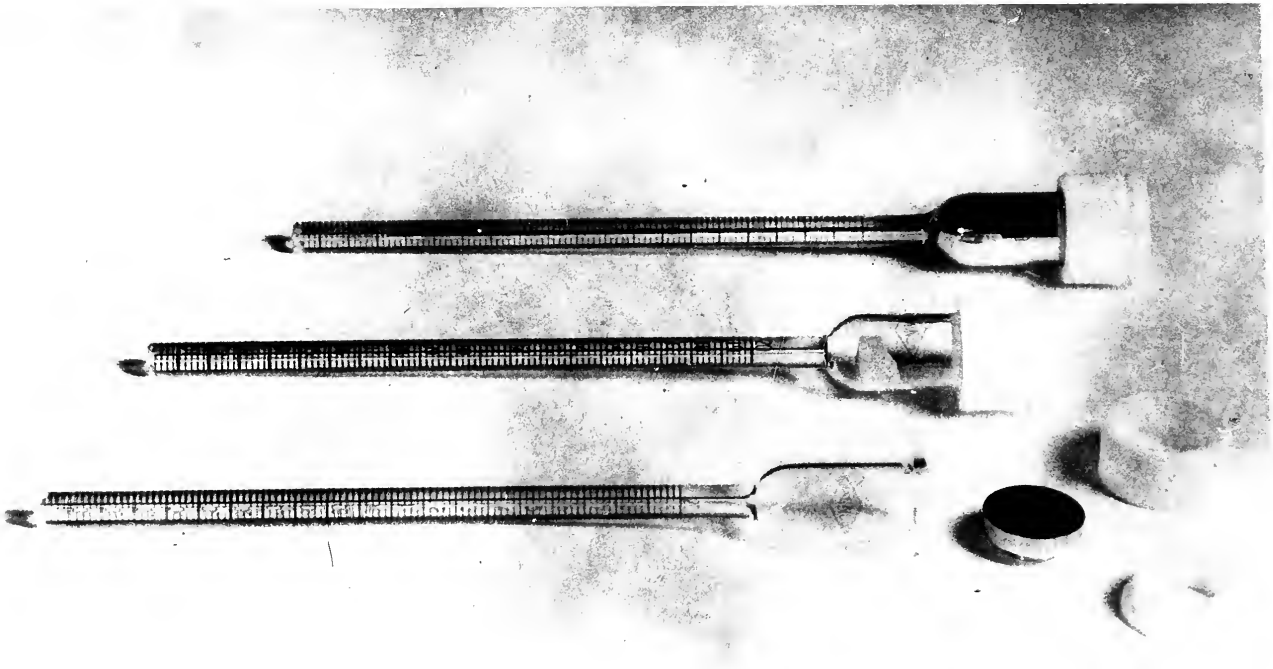

Figure 1

Penetrometers:
Disassembled, Assembled with Sample and Filled with Mercury

about ± 0.5% of the full scale reading.

While in the instrument intrusion of mercury is sensed by a stainless steel needle which follows the position of the meniscus of the mercury in the capillary stem of the penetrometer. A circuit is arranged such that, when closed, it includes the mercury and the needle. When the surface of the mercury moves the circuit is opened and an electric motor is actuated to drive the needle back into contact with the meniscus. As the needle advances its movement is registered by a counter on the front of the instrument. The linear movement of the needle is recorded digitally on the counter in terms of volume of mercury intruded. The smallest change in volume which can be registered is 0.00005 ml.

Several modifications were effected on the commercially-supplied instrument. The apparatus supplied for the purpose of filling the penetrometer with mercury and for making intrusion measurements at pressures less than one atmosphere was removed, because use of this apparatus necessarily involved an operation which could result in a partial removal of mercury already intruded into the sample. The extent of this inherent error could not be determined. Also, the metal back of the instrument was discarded as it led to a build-up of heat in the pressure vessel and the entire electric/hydraulic pump unit was removed from the cabinet and relocated nearby for the same reason. In addition, a solenoid valve necessary to the generation of pressure was moved outside the cabinet as it caused an objectionable jerk when it fired.

Instead of the commercial apparatus for filling the penetrometer and for low pressure intrusion measurements, a filling device* of original

* U. S. Patent Application 583,838, Prado Laboratories, Inc., Cleveland, Ohio.

design was used. This device is shown in Figure 2. Reference will be made to the letters on the figure.

The device is essentially a long glass tube divided into two chambers, C and G, by a constriction, E. The closed end of chamber C is formed into a bullet nose, A. A side arm, B, is joined to chamber C as is a smaller glass tube and greaseless Teflon stopcock, D. Chamber G can be opened with a ground joint, F. Another tube and standard stopcock, H, are located at the closed end of chamber G. The entire assembly is mounted so as to permit rotation about the long axis of the main tube, G and C. Tube and cock D are used for adding mercury to the device while tube and cock H are for evacuation and admission of air to the device.

The filling device is connected to a vacuum manifold as shown in Figure 3. This manifold also includes an absolute manometer capable of registering one atmosphere, a tilting McLeod gauge, a mechanical vacuum pump and a fine needle valve to admit controlled increments of air to the entire system.

Technique for Measurement of Mercury Intrusion

All samples which were tested in the porosimeter were dried by one of the previously described methods. Samples were tested in the bulk state and not ground as for sorption. A sample to be tested was broken from one of the cut sections of a cylinder. It was split off with a chisel and hammer with no special attention being given to obtaining a regular shape. The size of the sample selected was controlled by its pore volume. The instrument is only capable of measuring a pore volume of 0.2 ml. This constraint acts to limit sample size to ranges between 0.25 gms and 1.0 gm depending on age and water:cement ratio.

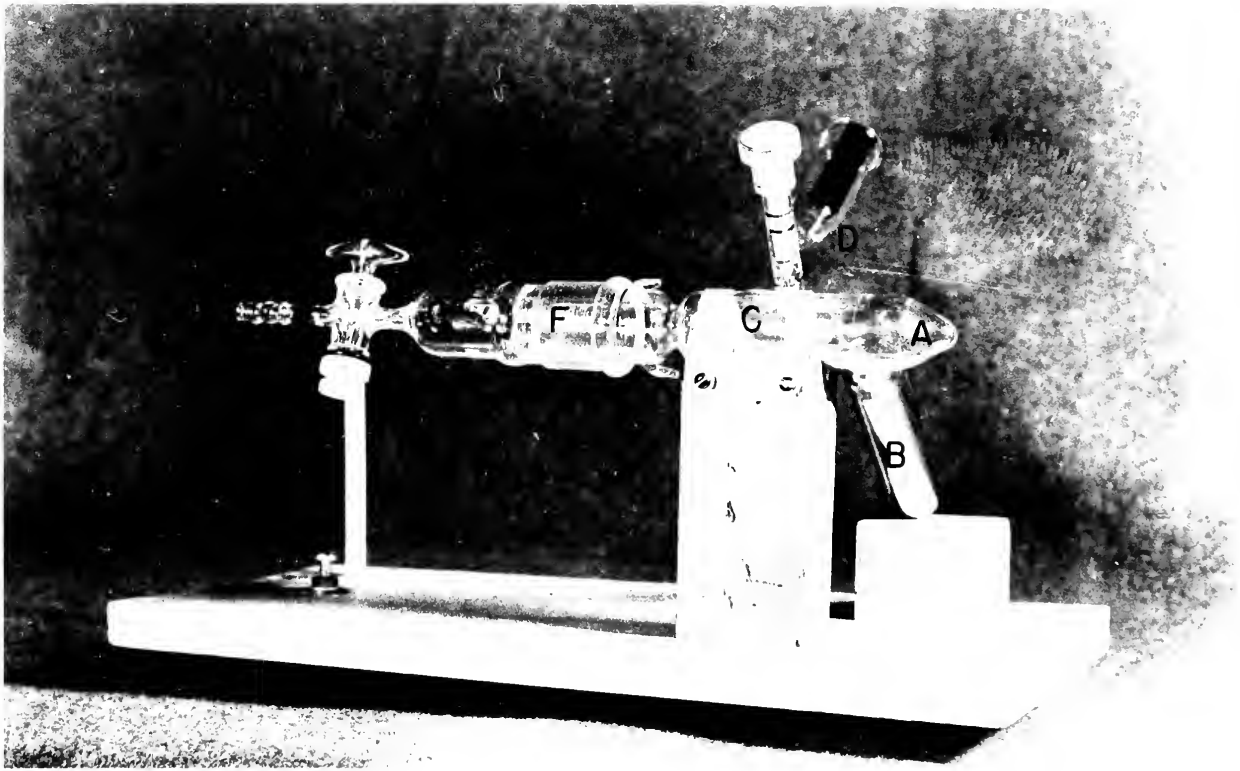

Figure 2

Filling Device

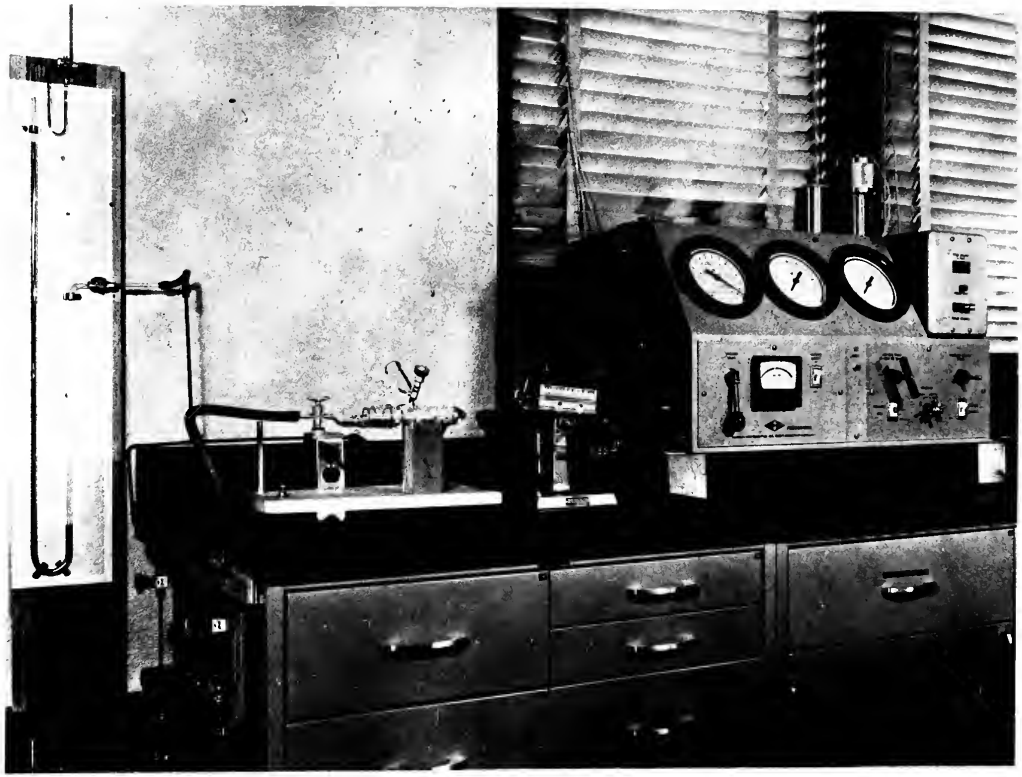

Figure 3

Porosimeter and Filling Device
with Related Equipment

The operation of the porosimeter involved the following steps: A sample of appropriate size was weighed and placed in the sample bulb of the penetrometer, and the closure assembled. See Figure 1. The penetrometer and sample were then reweighed. A small one hole stopper made of Teflon was slipped over the capillary stem and slid down the stem to a position near the sample bulb. The stopper was split at one place in the direction of the long axis. When it was in place along the capillary this split was slightly open.

The filling device was opened at the ground joint and the penetrometer inserted stem first. When in position the open end of the capillary stem rested in the bullet nose. The stopper pressed against the constriction and the split in the stopper was pointing approximately straight up. The split provided communication for gas through the constriction. The cap was then replaced over the sample bulb end of the penetrometer. A wad of glass wool in the cap kept the penetrometer pressed against the constriction. The entire manifold and the filling device were then evacuated.

In use the side arm of the filling device acts as a reservoir for mercury. By rotating the device so that the side arm rises the level of mercury in the main tube goes up as mercury empties from the side arm. Rotating in the opposite direction lowers the mercury level as mercury reenters the side arm.

At the beginning of a test the side arm was in the down position and was full of mercury, and a puddle of mercury lay in the main tube. The constriction confined the mercury to one end of the main tube. As mercury was placed in the penetrometer and removed from the filling device

during each test it was necessary to replenish the supply at the beginning of the following test. This was done by admitting the required amount of mercury to the filling device through the Teflon stopcock located between the constriction and the bullet nose. Generally this brought the level of mercury in the long tube to just below the stem of the penetrometer.

The level of the filling device was then checked. This was done by rotating it slightly and ensuring that the surface of the mercury came in contact with the entire capillary stem at the same time. If it did not the device was brought into level. The system was then allowed to evacuate to the desired pressure. Any reasonably low pressure was satisfactory providing that it was known. Generally the system was evacuated to 5 to 15μHg. The filling device was then rotated so that the level of mercury rose and covered the open end of the penetrometer and it was blocked in this position.

The vacuum pump was then isolated from the system, and a small increment of pressure was admitted via the fine needle valve connecting the system and the atmosphere. The capillary stem acted as a large pore and a pressure of about seven millimetersHg was required to intrude it. Hence, this first increment was at least seven millimetersHg. As soon as the stem was intruded the sample bulb was also filled. When this had occurred, the filling device was rotated down so that the tip of the capillary stem was no longer immersed in the mercury and the filling device was blocked in this position.

At this point the entire penetrometer was flooded with mercury. In addition, any large pores in the sample were also filled. Thus, the maximum

diameter of a pore which could be included in the distribution to be measured was fixed by this first pressure increment. All larger pores were filled and lost to measurement. Since it was found that even the youngest cement pastes had no very large pores, the determinations were generally begun at a pressure higher than seven millimetersHg. Usually, a pressure of 30 mmHg was used which filled all pores larger than about 210μ in diameter.

The pressure was then increased and held at some higher level and the corresponding change in the position of mercury in the stem noted. This process was repeated until the pressure in the system reached one atmosphere. This pressure corresponded to a diameter of about 8.5μ. Since the cement paste samples tested had essentially zero pore volume above 8.5μ, the pressure was raised to one atmosphere in one step instead of many.

The filling device was then opened and the penetrometer removed and weighed (without the Teflon stopper). The volume of mercury in the penetrometer was obtained from the full and empty weights of the penetrometer and the density of mercury.

The penetrometer was then placed, stem down, in the pressure chamber of the high pressure porosimeter and the chamber closed. A small vent at the top of the chamber was left open. The electric pump was used to completely fill the chamber with alcohol. When it was filled the pump was stopped and the vent closed. It should be noted that since the capillary stem was down the sample was under a pressure less than atmospheric. The probe used to sense the position of the mercury in the penetrometer stem was then actuated.

Next the pressure was raised to some desired level and held until the counter ceased to show a change in the mercury position. This equilibrium point was taken to be when the counter registered a change in volume of less than 0.0001 ml in one minute. Experiments showed that further refinement of the concept of equilibrium produced no real change in the resulting pore size distribution curve.

Generally, the pressures to which the system was raised were preselected. They were picked so that they could be read on the gauges without need for interpolation between markings on the gauges. Also, they were selected to give reasonably spaced points on the pore size distribution curve. The process of raising the pressure and holding it until mercury movement ceased was repeated until the pressure had reached 15,000 psi. Generally, six to twelve increments were used for each test. Successive tests on the same material were run with different pressures so as to yield data points falling between those obtained in the first test.

At the conclusion of a test the probe was returned to its down position, the pressure was released, and the penetrometer removed from the pressure chamber. All mercury recovered from the penetrometer was cleaned under nitric acid and filtered before being reintroduced into the filling device.

Reduction of Data to Pore Size Distributions

When a pore size distribution is determined by mercury intrusion the basic data that are recorded are pressure and volume of mercury intruded. The pressure that must be recorded is the absolute pressure on the sample. The apparent volume of intruded mercury that is read during the test is

subject to several corrections and the volume of intruded mercury that is finally recorded is the corrected volume.

While not a correction to raw data certain aspects of the geometry of the porosimeter and the way in which pressures were measured dictated adjustments in the pressure applied. The method utilizes the absolute pressure applied to the sample. While in the filling device the pressure on the sample was exactly that registered by the manometer. However, in the pressure cell of the porosimeter, the sample holder was held vertically with the open end of the stem down. Thus, the pressure on the sample varied from that applied to the mercury by this negative head. Further, the gauges on the instrument showed zero pressure when exposed to one atmosphere. So, the absolute pressure on the sample became the gauge pressure plus one atmosphere less the negative head. This usually meant adding about 11 psi to the gauge pressure to obtain the absolute pressure at the sample.

When the sample holder is initially filled with mercury, air at the very low pressure of evacuation is trapped in it. Further pressuring results in the compression of this air and this compression is included in the measured gross intruded volume. The volume of this gas at the pressure of evacuation is equal to the volume of the inside of the sample holder less the volume of solid sample in it. This volume may be determined by measuring the volume of mercury which flooded the sample holder. Since, the initial pressure and volume are known, Boyle's Law can be used to obtain the volume of gas at any higher pressure. This results in a cumulative compression by which the gross volumes are reduced. This correction commonly amounted to about 0.001 ml total and its significance

was exhausted at a pressure of one atmosphere. However, it could easily be about 0.010 ml for a slightly lesser degree of evacuation.

The measured volume of mercury intruded must also be corrected for mercury compressibility. As the pressure is raised some mercury enters additional pores and also, all the mercury is compressed. The gross measurement of intrusion is actually the sum of these two things. For an accurate pore size distribution it is necessary to separate the two as only true intrusion is of interest.

To obtain the mercury compressibility a sample holder without a sample was loaded with mercury and a plot of the decrease in volume of this mercury with pressure was obtained. It should be noted that the compression measured in this manner is an effective and not a true compression. The glass sample holder also compresses and this results in a decrease in its internal volume. This change in internal volume has the effect of masking some of the true compression of the mercury because the mercury is forced back out of the stem by exactly the amount of the lost internal volume. An analysis of the elastic deformation of the sample holder showed that its change in volume plus the apparent compression of the mercury closely approached the "handbook" value for the compressibility of mercury. In any event it is only the apparent, or effective, compressibility that is of practical experimental importance.

The effective compressibility was then reduced to a plot of the fractional volume change of one milliliter of mercury versus pressure. Each test included the determination of the volume of mercury in the sample holder. Hence, the compressibility correction for each pressure simply involved calculating the volume change of the mercury actually present

from the unit volume plot and subtracting this volume change from the cumulative, measured intrusion. As a practical matter the maximum value of this correction varied between 0.0055 ml and 0.0065 ml for the tests here described.

It should be noted that upon compression mercury heats up as well as compresses. The expansion so caused tends to mask some of the compression and it is necessary to allow the mercury to return to its original temperature to truly measure the compression. In fact, pressuring to 1000 atm resulted in sufficient heat to mask more than 50% of the true compression and a pause of about 15 min was found to be required to allow the mercury to return to its starting temperature.

There is another compressibility factor for which no correction was made in this work. The compressibility of the sample is a function of its composition, pore structure and the amount of mercury already intruded into the sample. This extremely complex problem was not pursued.

An example of the corrections which were made follows. Suppose that a test is in progress and that at a gauge pressure of 789 psi the apparent intrusion is 0.0150 ml. The sample was evacuated to 0.005 mmHg, the pressure used to fill the penetrometer was 30 mmHg, and the volume of mercury which flooded the penetrometer is 6.1249 ml. The absolute pressure on the sample is 789 psi plus 11 psi or 800 psia. Boyle's Law shows that the loss in volume of the initially trapped gas is 0.0010 ml. At a pressure of 800 psia 6.1249 ml of mercury has compressed by 0.0003 ml. So, the true intruded volume is 0.0150 ml less 0.0010 ml (gas compression) and less 0.0003 ml (mercury compression) or 0.0137 ml true intrusion. Thus the recorded data are 800 psia and 0.0137 ml of intrusion. Of

course, the intrusion may be placed on a per gram of sample basis if desired.

With the use of the intrusion equation and the proper factor from Appendix B the absolute pressure is converted to a diameter. The cumulative pore size distributions are then merely a plot of these diameters and the corresponding volumes of mercury intruded.

Capillary Condensation

Apparatus for Capillary Condensation

All water vapor sorption measurements made in this work were done gravimetrically. That is, the amount of sorbed vapor was determined by measuring the change in weight of a sample exposed to the vapor. All weighing was done with an analytical balance. All sorption on Portland cement paste was done in aluminum desiccators which were about 30 cm in diameter and 30 cm high and were fitted with standard glass vacuum desiccator lids. The liquid used to control the partial pressure of the water vapor was placed in the bottom of the desiccators and was continuously stirred with magnetic stirrers. The Portland cement samples were placed in low-form weighing bottles which were about 30 mm high and 60 mm in diameter. In use, the weighing bottles rested on a perforated plate in the desiccator about 75 mm above the level of the liquid.

Capillary Condensation Measurement Technique

A solution of glycerol and water was used to control the partial pressure of the water vapor in the desiccators. The method of controlling partial pressures is that found in ASTM Recommended Practice E 104-51. The partial pressure is controlled by the concentration of glycerol in

the solution. The concentration is measured indirectly by measuring the refractive index of the solution. The ASTM method directly relates the partial pressure and the refractive index. Technical grade glycerol was used except in cases where a very low partial pressure was desired. In these cases it was necessary to use reagent grade glycerol to obtain a solution with a sufficiently low water content. Refractive indices were measured with a refractometer* which met the specifications of E 104-51.

Samples on which water vapor sorption data was desired were selected as described earlier. They were then oven dried at 105°C. When drying these samples, the oven was continuously evacuated to a pressure of one micron. Thus, the samples were exposed to a minimum amount of air during drying. After drying the samples were ground in a mortar and pestle until they passed a No. 60 U. S. Standard Sieve which had 250μ openings. After grinding the samples were redried in the vacuum oven as above.

Approximately 1500 ml of solution with the desired partial pressure was prepared and placed in the bottom of the desiccator. The dry powder samples were placed in preweighed weighing bottles and weighed again. Then they were placed in the desiccator, their tops removed and the desiccator closed. Approximately one gram of sample was put in each bottle and no less than three duplicate bottles were tested. The desiccator was evacuated to the pressure controlled by the liquid, and left in a constant temperature room. During sorption the solution was stirred continuously with a magnetic stirrer.

Sorption was allowed to proceed for exactly 24 hours, for reasons which will be discussed later. Then the desiccator was opened and the bottles were recapped and reweighed. For each partial pressure a

* Karl Zeiss Model 37426.

completely moisture-free sample was used and the above process repeated. Thus, all samples for all partial pressures started out completely dry and were allowed to sorb water for exactly the same length of time.

Calculation of Pore Size Distribution for Condensation Data

The above measurements yielded the water vapor sorption isotherms shown in Figures 4 and 5. The amount of water sorbed was taken to represent the combined effects of capillary condensation and sorption on surfaces. That is, water vapor condenses in pores smaller than some diameter controlled by the partial pressure, while on all other surfaces a layer of sorbed water exists. One would like to be able to relate a change in amount sorbed between two partial pressures to the volume of pores existing between the two corresponding pore diameters. However, the change in sorption between two partial pressures on the experimental isotherm cannot be used to get this value directly since as the partial pressure is changed some additional vapor is sorbed onto or off of surfaces not yet covered by capillary condensation.

For this reason it is necessary to know the amount of vapor sorbed on a non-porous surface as a function of partial pressure and the non-porous surface must be as similar as possible to the surface of the porous material. Such a sorption isotherm for a non-porous material is called a "t-curve" (for thickness) and is generally shown with the thickness of sorbed vapor, rather than the sorbed volume, plotted against partial pressure. In this work a t-curve was measured for water vapor on crushed quartz. A complete discussion of the experimental procedure and results are to be found in Appendix C.

With the water vapor-cement paste isotherms and the t-curve, pore

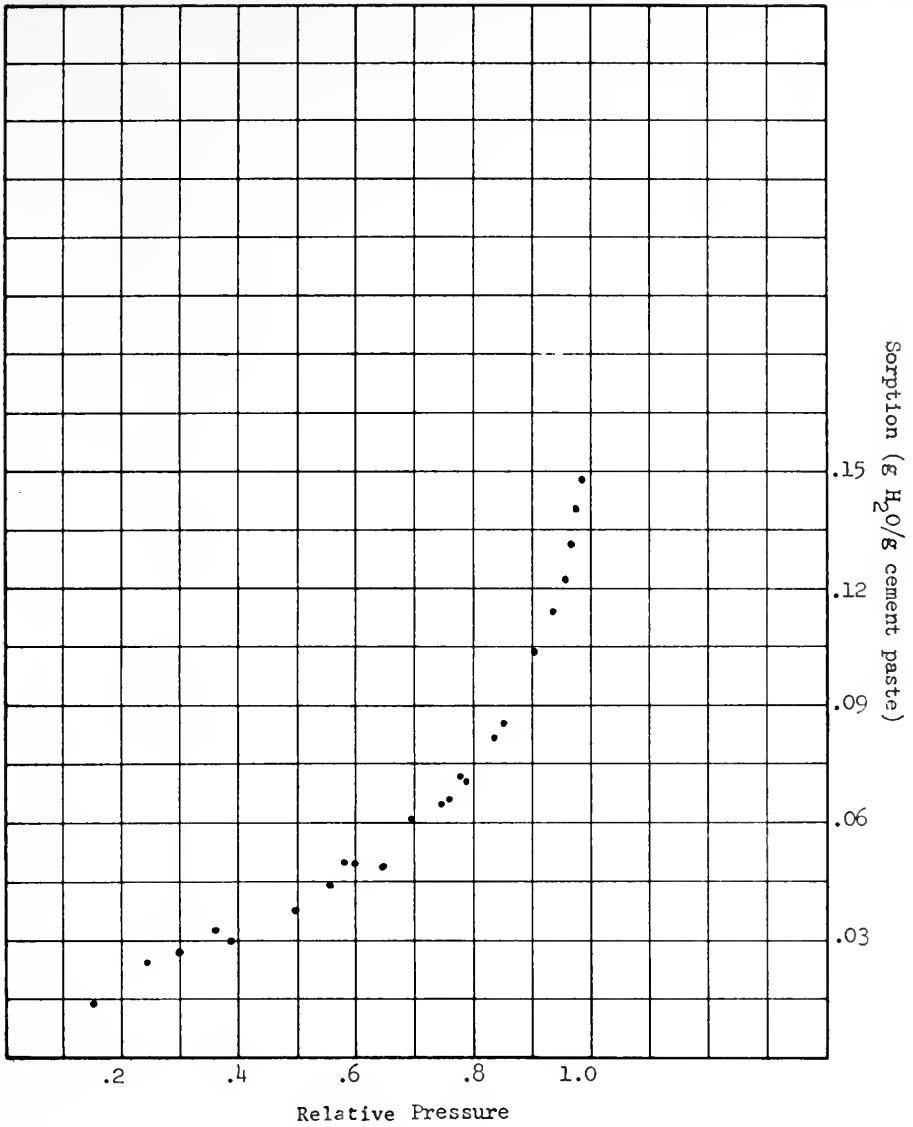

Figure 4

Water Vapor Sorption Isotherm
for Cement Paste at 28°C
(water:cement ratio 0.4)

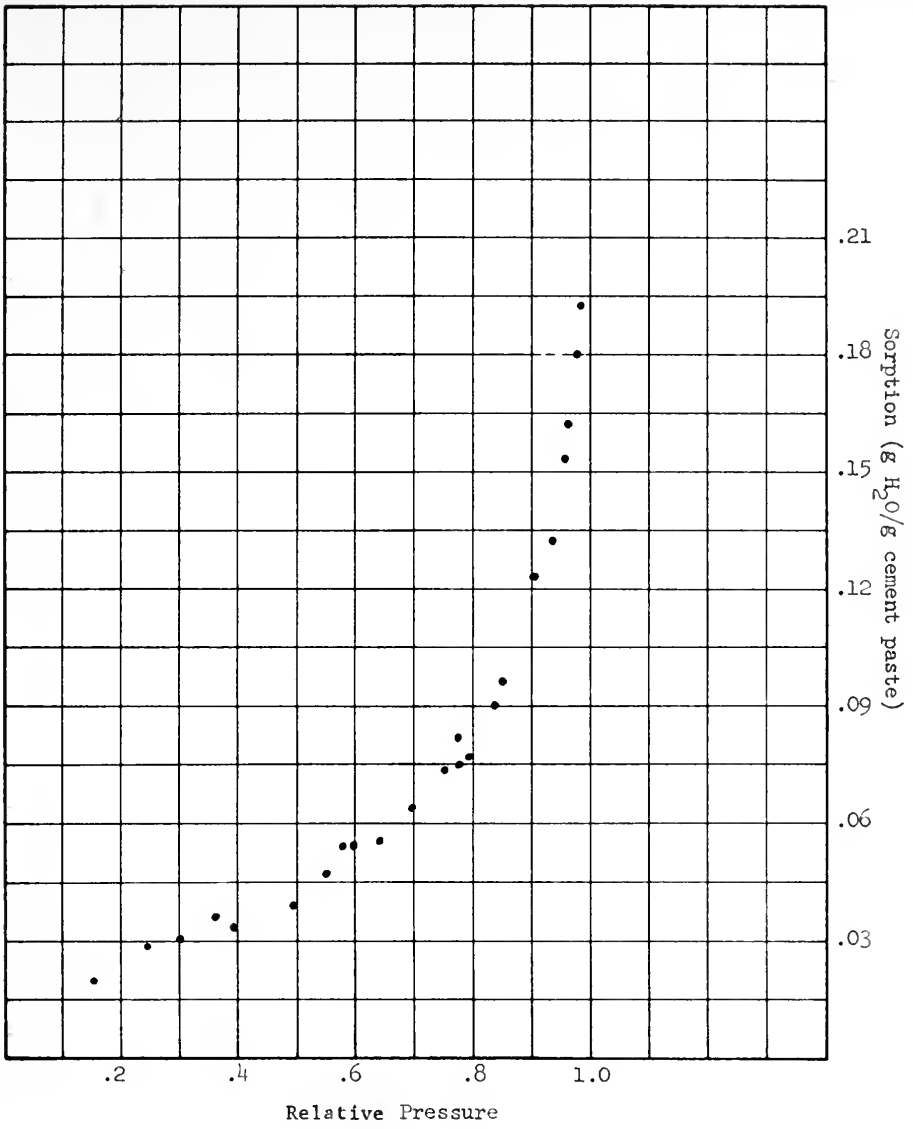

Figure 5

Water Vapor Sorption Isotherm
for Cement Paste at 28°C
(water:cement ratio 0.6)

size distributions were calculated. The method of Roberts (18) was used. The method recognizes that, temporarily disregarding capillary condensation, a layer of vapor will exist on all pore walls and that the thickness of this layer will be a function of partial pressure. If capillary condensation occurs in a pore then the diameter is given by the Kelvin equation, and this diameter is the actual diameter of the pore less twice the thickness of the sorbed layer on the pore walls. In other words, the diameter that the condensing vapor "sees" is the diameter of this inner core and differs from the true diameter by the thickness of already sorbed film. With this recognition the Kelvin equation and the t-curve are used to convert the partial pressure abscissa of the isotherm to an abscissa showing directly the true pore diameter.

Given a t-curve and preselected pore diameters it is possible to calculate essentially geometric factors which reduce the measured amount of vapor sorbed by the amount which reflects the thickening of the layer of vapor on pore walls in which condensation has not occurred. Roberts' method is an orderly way of computing and keeping track of these factors. A table of these factors is generated and then applied to the isotherm with the corrected abscissa.

The Kelvin equation is the fundamental tool used to obtain a pore size distribution in this method. The geometric correction factors and the t-curve might be viewed as merely correcting the data for certain unavoidable experimental phenomena so that the Kelvin equation will yield the proper pore diameter and pore volume.

RESULTS

Effect of Atmospheric Exposure

Exposure of cement paste samples to the atmosphere could result in carbonation and an attendant change in the pore size distribution. Mercury intrusion pore size distributions were measured for companion samples which differed only in that one of the samples had been exposed to the laboratory atmosphere for a period of three weeks and the other sample had not. No difference was noticeable in the mercury intrusion pore size distributions of the two samples.

Effect of Drying Technique

Appendix B discusses the method used to measure the intrusion equation factor for cement paste which has been "P" dried and oven dried. The factors were found to be 179μlbs/in^2 for "P" drying and 123μlbs/in^2 for oven drying. Figure 6 shows that, even when the applicable factor is used, two companion samples, differing only in drying, exhibit differences in pore size distributions.

Equilibrium Times for Intrusion of Mercury

Figures 7 and 8 show the time required for a unit volume of mercury to intrude and come to equilibrium in cement paste as a function of pore diameter. Several water:cement ratios and ages are illustrated. Comparison of these with the appropriate pore size distributions in Figures 9 and 11 show that the maximum time for equilibrium occurs at that point

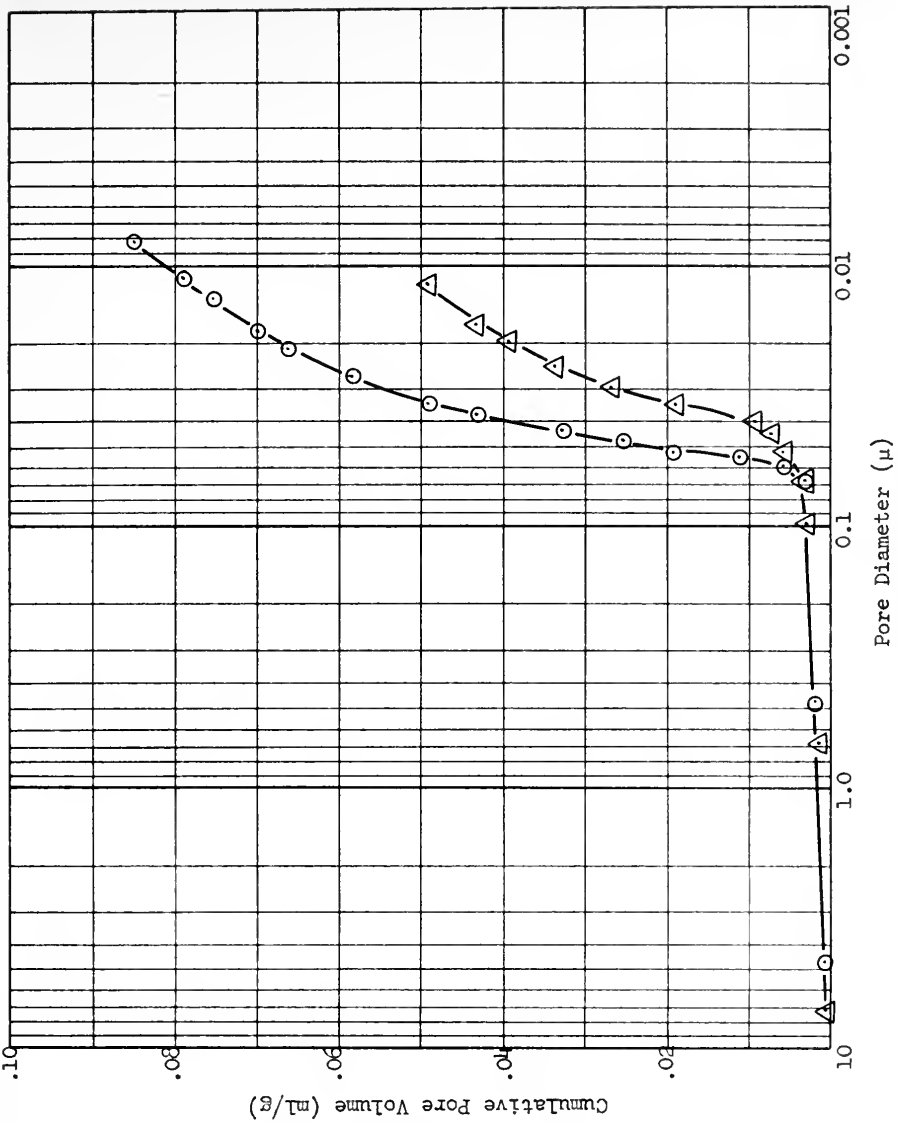

Figure 6

Mercury Intrusion Pore Size Distributions
for Replicate Cement Pastes
"P" Dried (△) and Oven Dried (⊙)

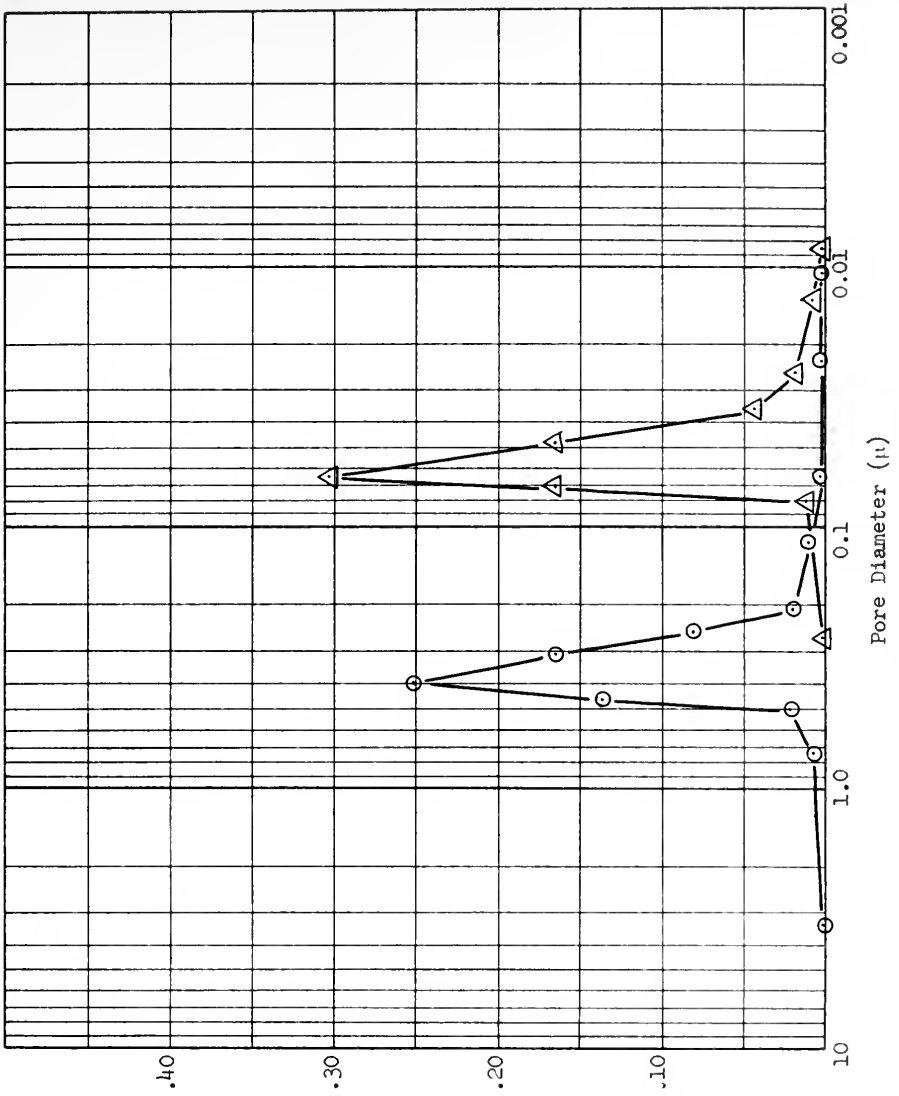

Figure 7

Time to Reach Equilibrium
for Mercury Intrusion in Cement Pastes
at Ages of 2 days (⊙) and 320 days (△)
(water:cement ratio 0.4)

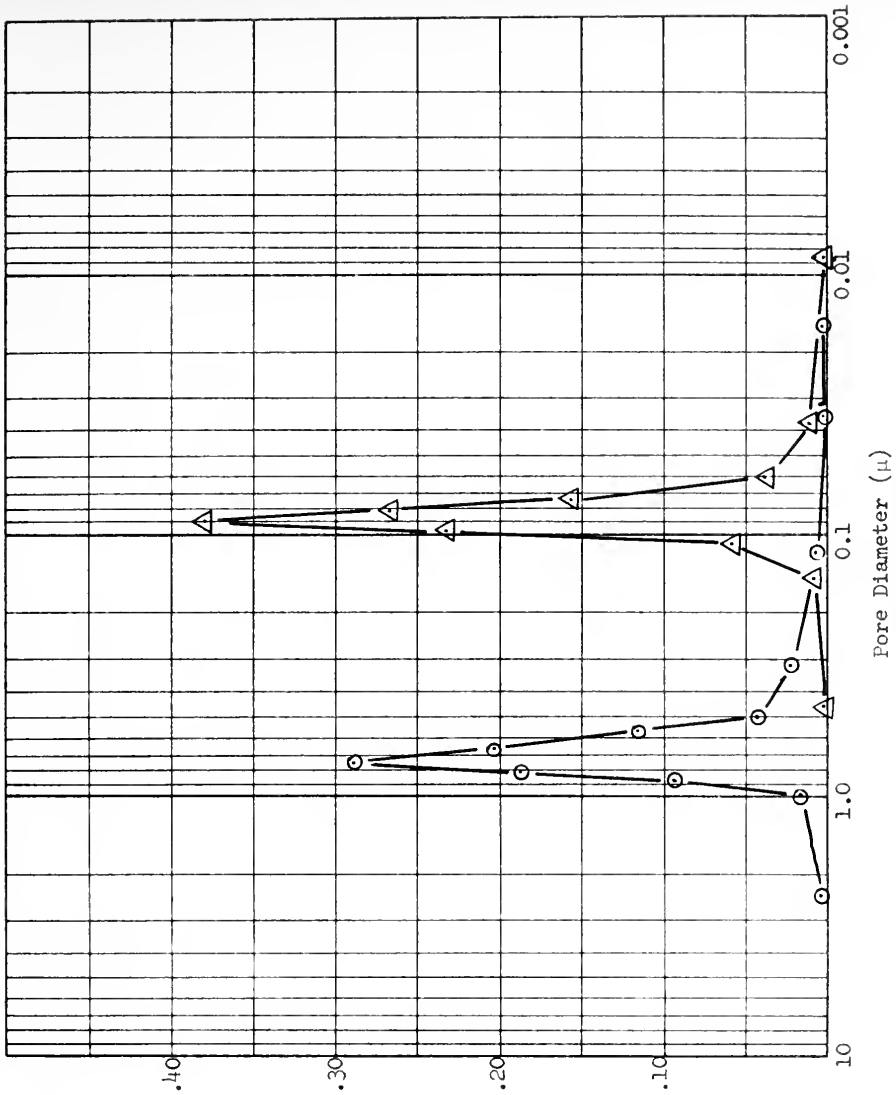

Figure 8

Time to Reach Equilibrium
for Mercury Intrusion in Cement Pastes
at Ages of 2 days (⊙) and 318 days (△)
(water:cement ratio 0.6)

in the pore size distribution where the initial significant intrusion is taking place.

Evolution of Pore Size Distributions

Figures 9, 10, 11 and 12 show the mercury intrusion pore size distributions for water:cement ratios of 0.4 and 0.6 for ages varying from one day to about one year. For clarity, the distribution curves are shown without specific data points. All pore size distributions are plotted both as a function of volume of pores per unit weight and as a function of percent of total pore volume. Complete and specific data for each pore size distribution determination are to be found in Appendix D. Duplicate pore size distribution curves, with specific data points, for some of the samples are to be found in Appendix E.

Equilibrium of Water Vapor Sorption

The time rate of sorption of water vapor on cement paste was examined and the results are shown in Figures 13 and 14. No true equilibrium was found for the cement pastes used in this research. However, a sharp break in the rate curves is to be seen after about 24 hours. This was taken to be the point at which capillary condensation ceased and, hence, data for pore size distributions was taken at 24 hours.

Comparison of Pore Size Distributions by Mercury Intrusion and Capillary Condensation

Figures 15 and 16 show pore size distributions for cement pastes of two different water:cement ratios at one age. Each figure shows the distributions obtained by both mercury intrusion and capillary condensation of water vapor for replicate samples. The capillary condensation pore

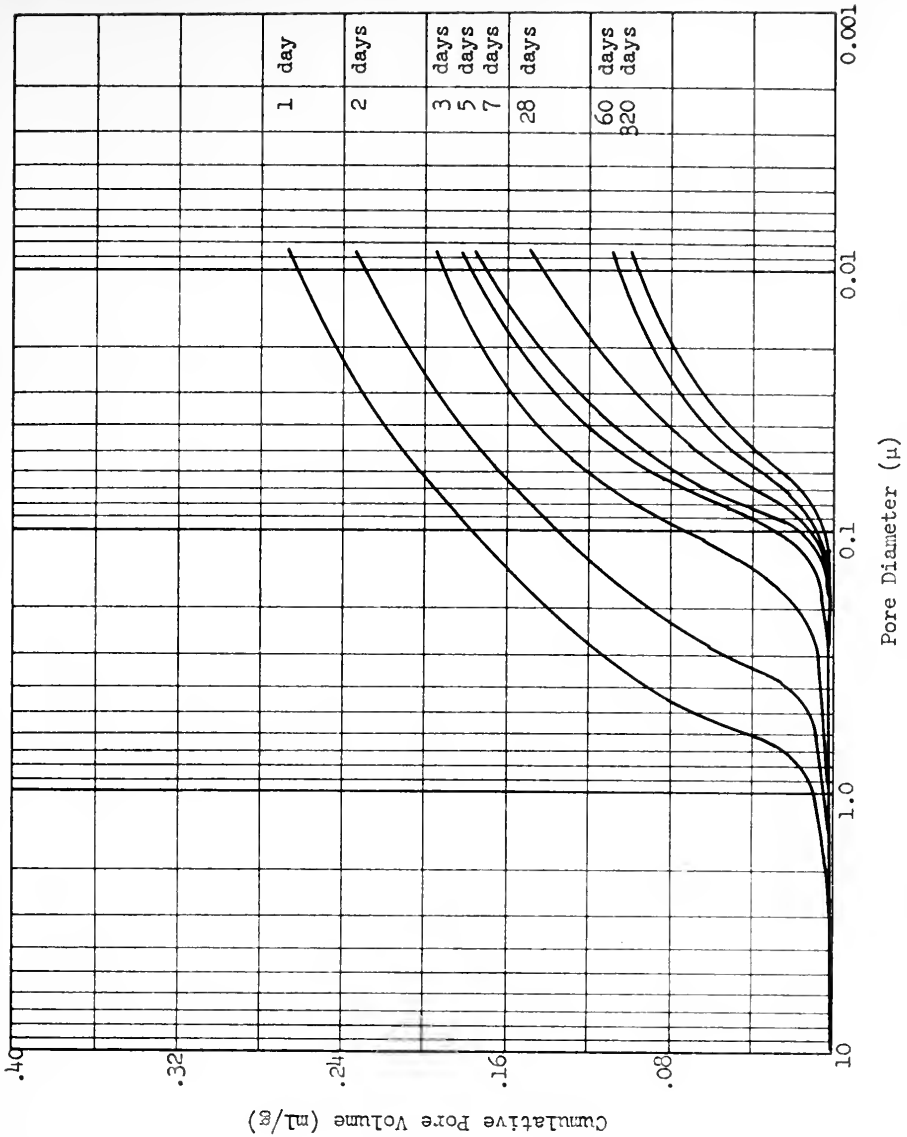

Figure 9

Mercury Intrusion Pore Size Distributions
for Cement Pastes at Eight Ages (water:cement ratio 0.4)

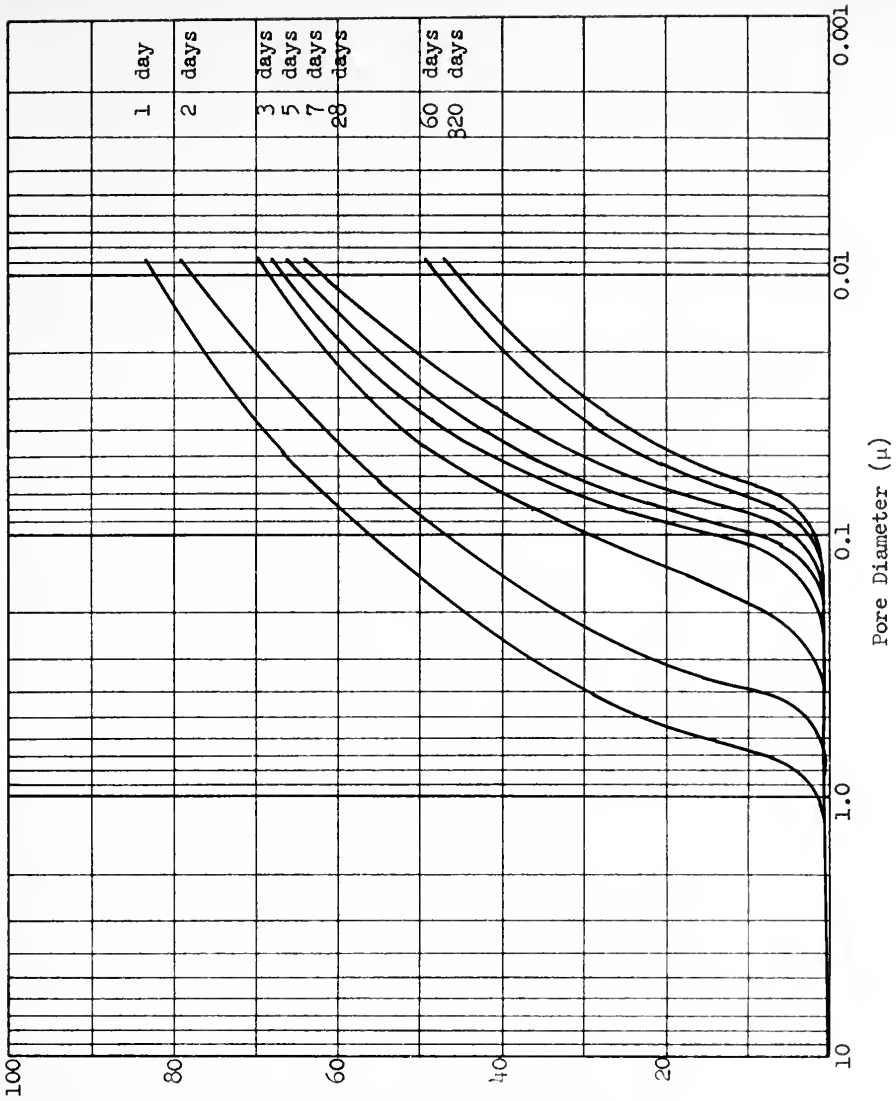

Figure 10

Mercury Intrusion Pore Size Distributions
for Cement Pastes at Eight Ages (water:cement ratio 0.4)

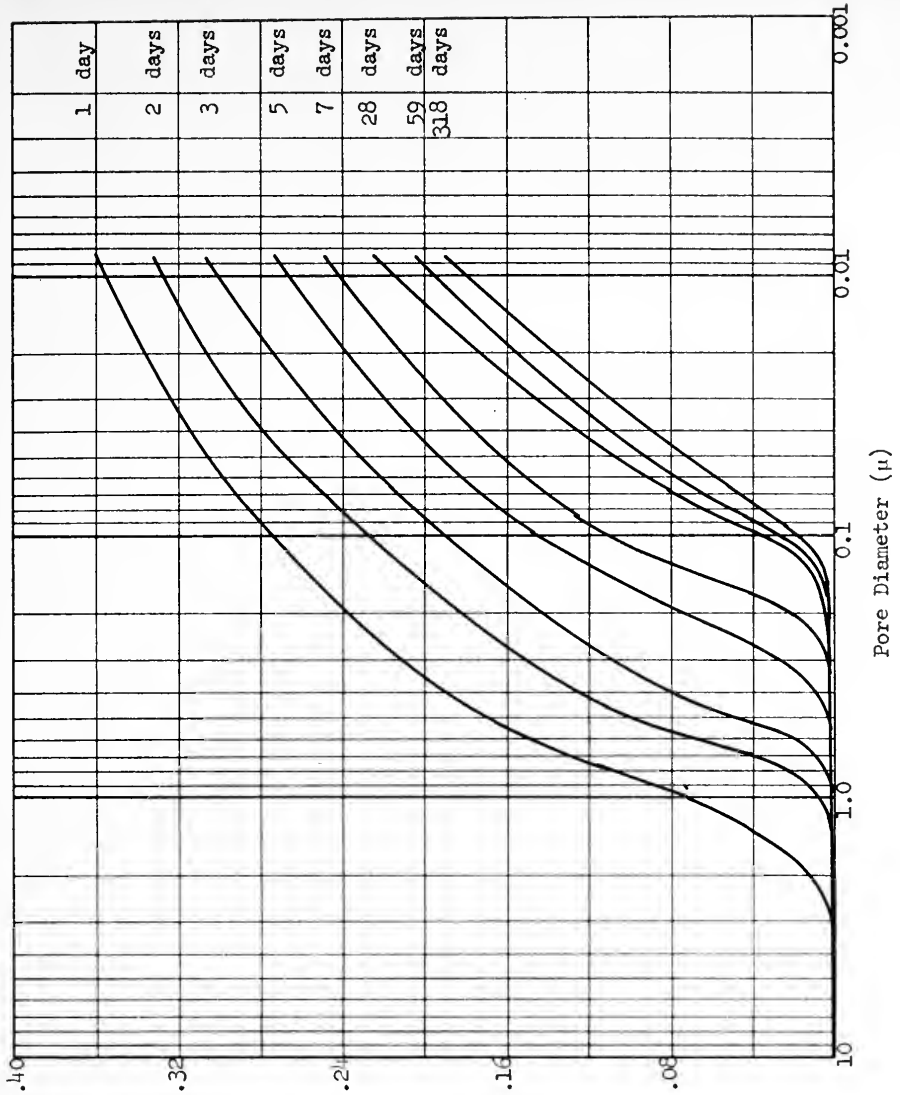

Figure 11

Mercury Intrusion Pore Size Distributions
for Cement Pastes at Eight Ages (water:cement ratio 0.6)

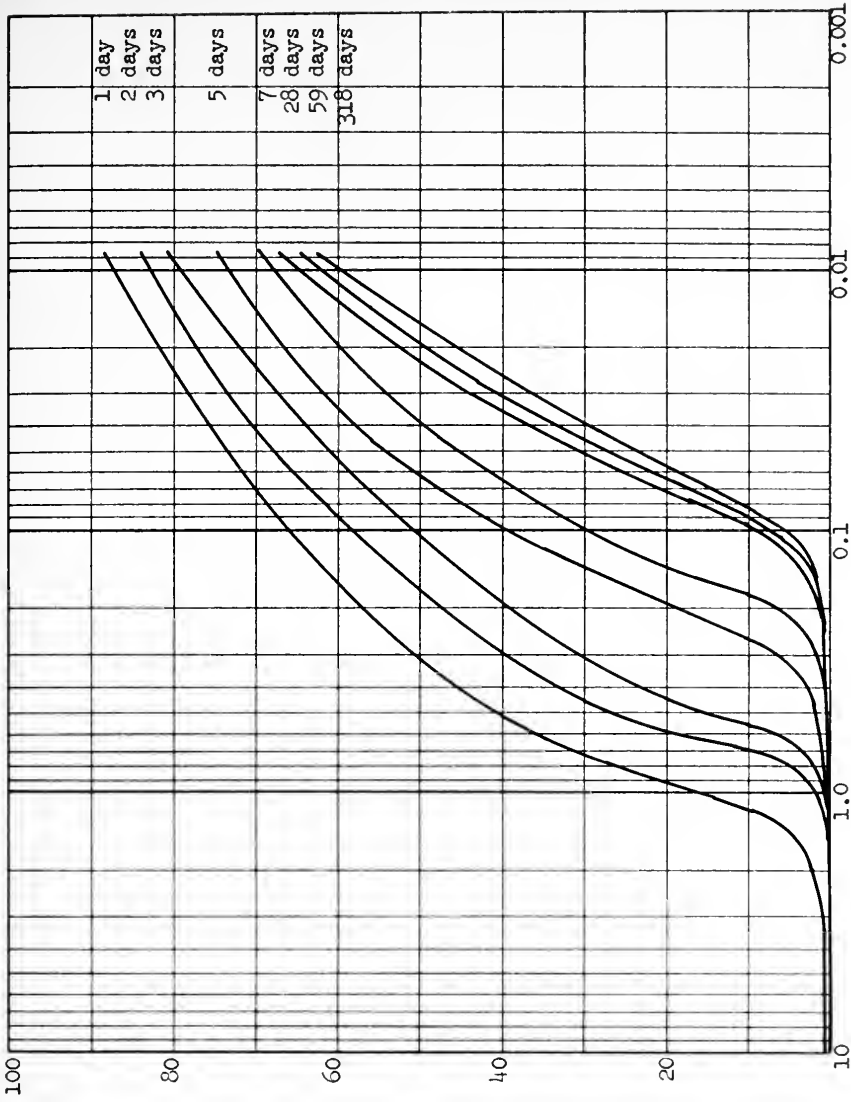

Figure 12

Mercury Intrusion Pore Size Distributions
for Cement Pastes at Eight Ages (water:cement ratio 0.6)

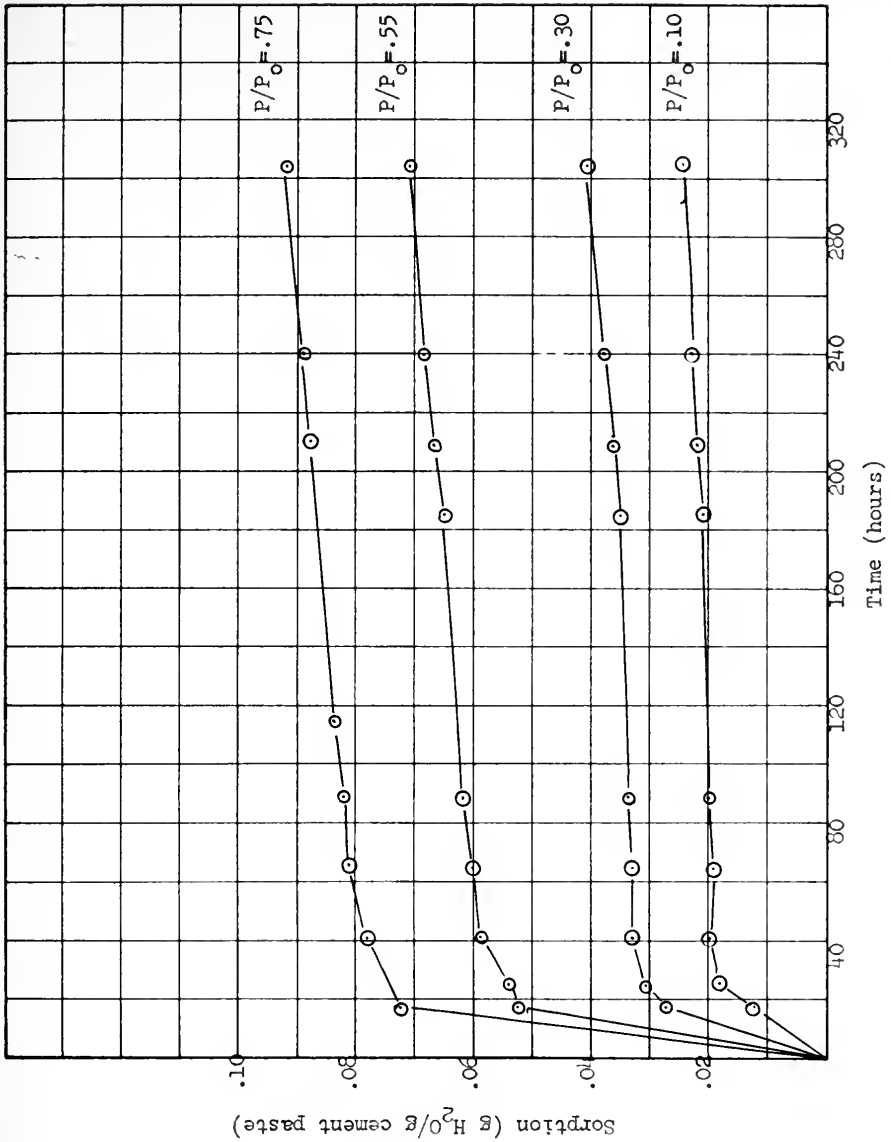

Figure 13

Time Rate of Sorption
of Water Vapor on Cement Paste
at Four Partial Pressures
(water:cement ratio 0.4)

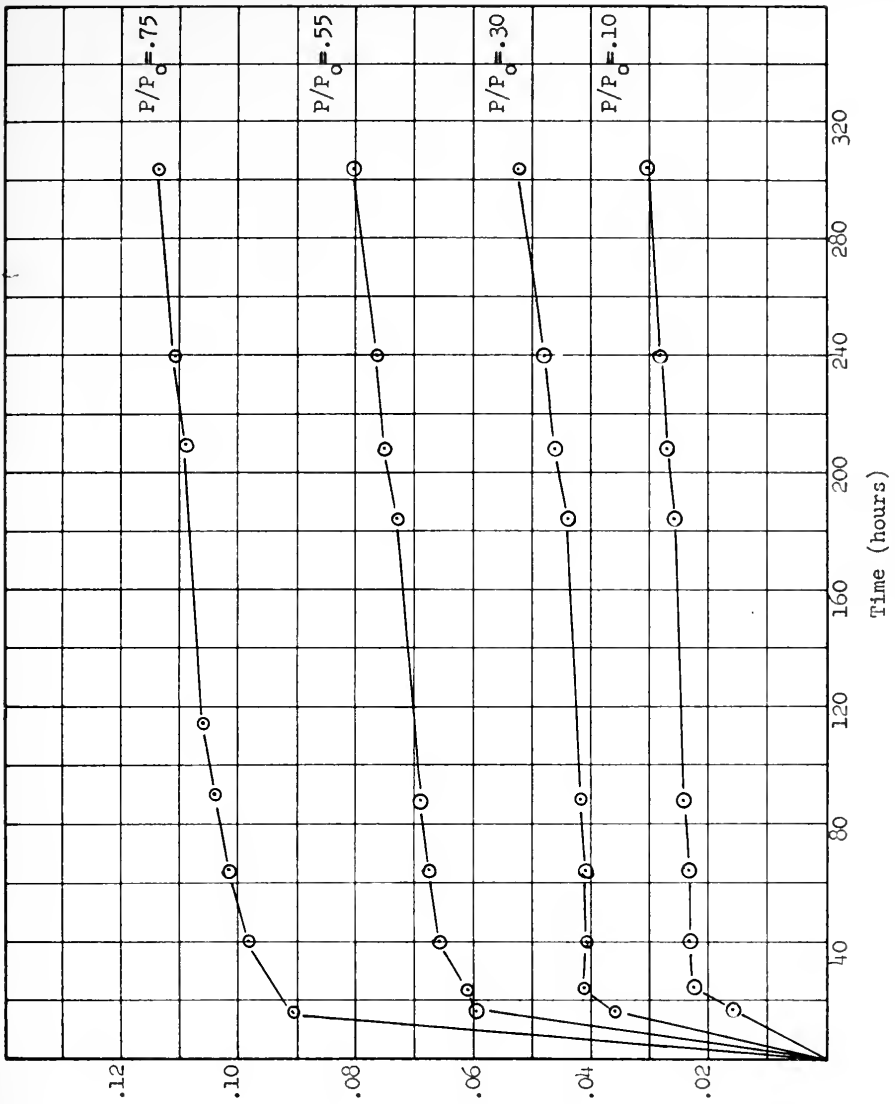

Figure 14

Time Rate of Sorption
of Water Vapor on Cement Paste
at Four Partial Pressures
(water:cement ratio 0.6)

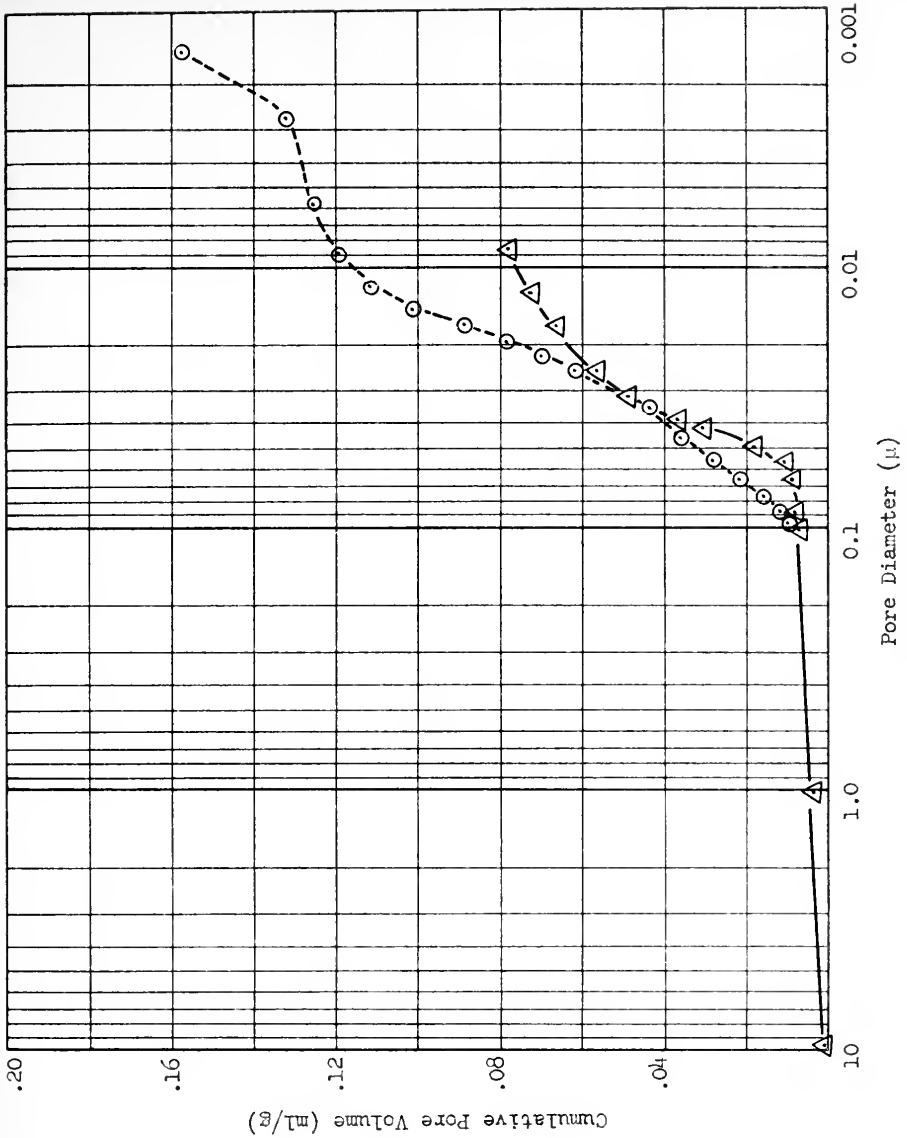

Figure 15

Comparison of Pore Size Distributions
on Replicate Samples of Cement Paste
Using Water Vapor Sorption (⊙) and Mercury Intrusion (△)
(water:cement ratio 0.4)
(age = 267 days)

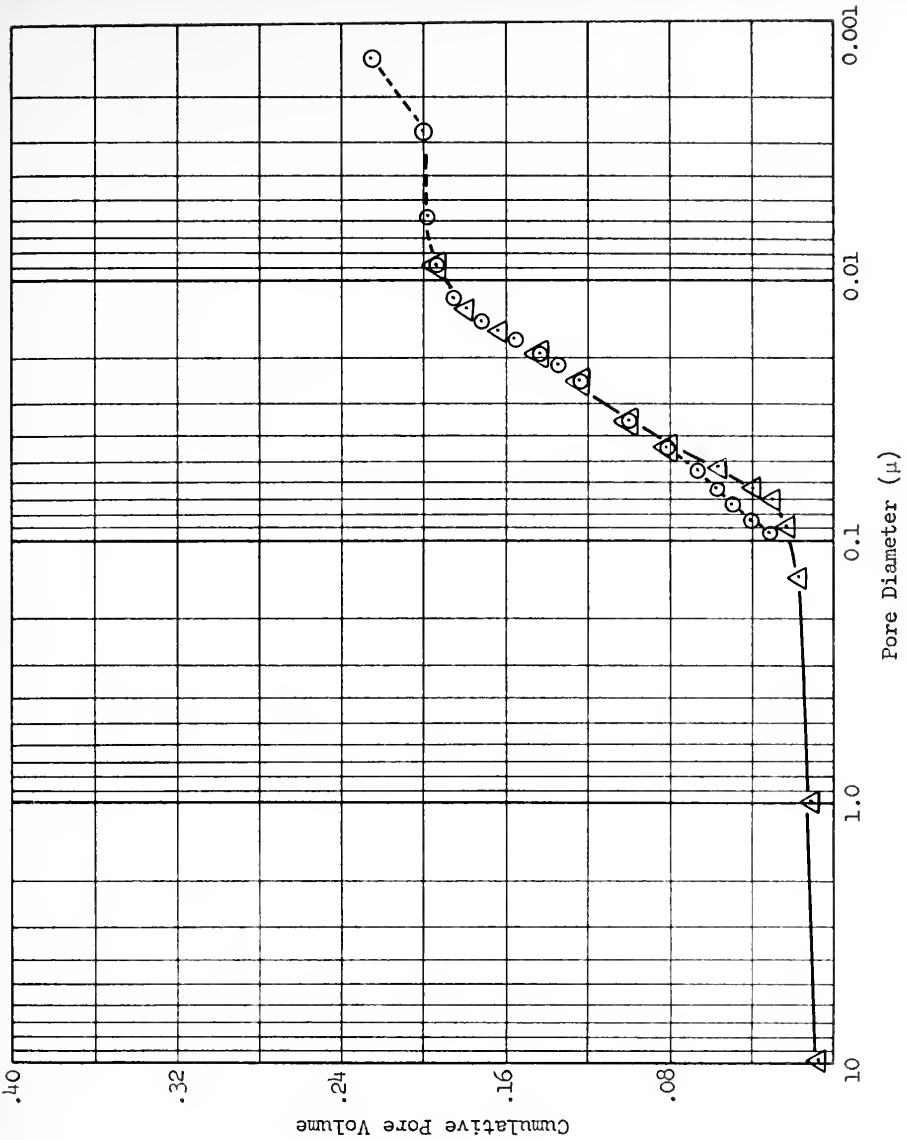

Figure 16

Comparison of Pore Size Distributions
on Replicate Samples of Cement Paste
Using Water Vapor Sorption (⊙) and Mercury Intrusion (△)
(water:cement ratio 0.6)
(age = 267 days)

size distributions which are shown are really composite ones. Capillary condensation only provided data in the range 0.1μ diameter to 0.0014μ diameter. The capillary condensation distributions were added onto the small volume of pores with diameters greater than 0.1μ that was measured by mercury intrusion. The pore size distributions for both water:cement ratios show that water vapor sorption measures a greater pore volume in the pore diameter range 0.1μ to about 0.05μ or 0.04μ. For diameters less than this, the two methods give excellent agreement in the case of the water:cement ratio 0.6 cement paste. In the case of the water:cement ratio 0.4 cement paste capillary condensation measures a greater pore volume for pore diameters less than 0.025μ. Specific data for both mercury intrusion and capillary condensation are to be found in Appendix G. The capillary condensation data are listed as measured and have not had the volume of pores with diameters greater than 0.1μ, as measured by mercury intrusion, added to them.

DISCUSSION

Experimental Matters

Several assumptions and experimental techniques used in this work directly effect the accuracy of the results that are presented. Before discussing the results then, the effect of these assumptions and techniques must be explored.

Method of Hydration

It should be recalled that all samples tested in this research were hydrated in a saturated solution of $Ca(OH)_2$. Thus, they were afforded the best possible environment for continued hydration prior to their removal for drying and testing. As a result it is to be expected that these samples have hydrated more, and consequently have lower pore volumes and less large pores, than cement pastes which are hydrated under less ideal circumstances.

Pore Shape Model

Both the technique of capillary condensation and mercury intrusion require the assumption of a pore shape model if the data is to be reduced to some representative pore size. In this work the pores are assumed to be cylindrical. No stipulation is made as to their length but they are assumed to be circular in cross section.

Examination of the scanning electron microscope pictures (Appendix F) of cement paste does not show truly cylindrical pores. Hence, the

diameters that are reported cannot be actual diameters of cylindrical pores. In fact, they are only representative sizes of irregularly shaped pores. Thus, a diameter of, say 0.05μ does not mean a cylindrical pore exists with a diameter of exactly 0.05μ but rather that there exists a pore with a cross section which has a representative linear dimension of about 0.05μ.

Process of Intrusion

At the outset of a mercury intrusion determination the sample is surrounded by mercury and no mercury is in the sample. As pressuring proceeds mercury flows through the sample's pores from the surface toward the center of the sample. Hence, the volume of an internal pore will be measured only when the mercury has intruded to it. If the pathway the mercury must follow to the internal pore is smaller in diameter than the internal pore then mercury will only fill this pore when it has been able to intrude the smaller pathway. As a result, any mercury intrusion pore size distribution is really a plot of the diameters of entryways against the volume of pores which are accessible through these entryways. This means that a pore size distribution obtained in this manner is really a lower bound on pore volume and that there may exist greater volumes of larger diameter pores than are shown because they can only be reached by smaller diameter pathways.

Effect of Atmospheric Exposure

Carbon dioxide and some or all of the constituents of Portland cement paste have been shown to react (20). In some cases, this reaction has led to considerable shrinkage of the cement paste and this reaction

could result in an alteration of pore size distribution of the cement paste.

All of the samples used in this research were exposed to the atmosphere for brief periods and a reaction between the CO_2 in the air and the samples was possible. Verbeck (20) has pointed out that carbonation occurs less readily in cement pastes of very high and very low moisture content. Further, he has shown that pieces of cement paste do not readily carbonate in their interior. Essentially all samples for this research were in the bulk state and were exposed to the atmosphere when either very wet or dry. Also, the periods of exposure were very brief. However, the oven dried samples were exposed to the atmosphere while they rapidly passed from high to low moisture content. Hence, the effect of possible carbonation on measured pore size distributions was assessed.

Some samples were deliberately exposed to the atmosphere for a period of three weeks. During this time they gradually passed from a high to low moisture content. It is believed that this exposure is more severe than any other samples received and that, if any samples were going to carbonate, these would be the ones. Comparison of mercury intrusion pore size distributions of these "carbonated" samples with companion pieces not so severely exposed showed no differences.

As a result of this work, it was concluded that the exposure to CO_2 that the samples in this research received did not alter their pore size distributions as measured by mercury intrusion. It should be recalled that the samples used for sorption studies were dried in a vacuum oven and were not exposed to the atmosphere while drying.

Effect of Drying Technique

When companion samples of cement paste were examined by mercury intrusion, it was observed that their pore size distributions differed when they were dried by different techniques. Since the distributions had about the same shape and were merely displaced along the pore diameter axis it was believed that the factor ($4\ \gamma \cos \theta$) used in the intrusion equation might be different for differing conditions of drying. The work in Appendix B indicated that this was indeed the case. However, even when the proper factors are used, pore size distributions on replicate samples do differ according to method of drying.

"D" dried replicates were also tested and their pore size distribution fell between those of the "P" dried and oven dried samples. Also, the water content of a "D" dried sample falls between that of an oven dried and "P" dried sample. Thus, it appears that some change in the apparent pore size distribution occurs upon variation of drying technique and that this change is related to the moisture content of the sample. The intrusion equation factor was only measured for the two extreme cases of "P" and oven drying so no "D" dried pore size distributions are reported.

Experiments showed that the change is completely reversible. If a sample is dried by any of the three techniques, resaturated and then redried by another technique, it will exhibit the same pore size distribution as if it had been originally dried by the latter technique. Thus, if an oven dried sample is rewetted and then, say "P" dried it will have the same apparent pore size distribution as a sample that has been only "P" dried.

The explanation for this phenomena is unknown. Oven drying was selected for all tests reported herein because it was the most efficient and because it afforded a measurement of smaller pore diameters at the same intrusion pressure because of its lower intrusion equation factor.

Assumption of Contact Angle

Appendix B discusses the direct measurement of the factor necessary to the reduction of mercury intrusion data. If it is assumed that the surface tension of the mercury is unchanged by the method of drying the cement paste then the contact angle between the cement paste and the mercury is seen to change appreciably and the drier cement paste exhibits a lower angle. Assuming a surface tension of 484 dyn/cm the contact angle for "P" dried paste becomes 129.6° and that for oven drying becomes 115.9°.

The contact angle is essentially the physical manifestation of the competition between the tendency of the liquid to remain as a discrete mass and the tendency of the solid to attract the liquid. As the tendency of the solid to attract the liquid becomes greater the contact angle is reduced. It is reasonable to expect that as the last bit of water (either physically or chemically held) is removed from the cement paste surface the tendency of the cement paste to attract some other molecule would be increased. Hence, it does not seem surprising that the contact angle is reduced.

It should be noted that a very small change in the water content of cement paste markedly affects the contact angle. Further, the proper contact angle appears always to be considerably lower than the contact angles (140° or 145°) which are usually assumed.

Equilibrium for Mercury Intrusion

During intrusion of mercury it was found that, at a rather narrow band of pore diameters, a unit volume of mercury required much longer to flow to equilibrium than at any other diameters. Of course, at very high pressures considerable time was required for equilibrium because of the already mentioned dissipation of the heat of compression of the mercury. However, this rate of dissipation was independently measured and could be subtracted from the measured equilibrium times. This correction accounted for the longer equilibrium times at high pressures but a peak in the equilibrium time curve still existed at a narrow band of diameters. This peak was always observed and always occurred at the diameter where the first really major intrusion was noted. Thus, it would seem that something is happening at this "threshold" diameter which causes a considerable slowing of intrusion.

Drake (5) briefly mentions the existence of this phenomenon for a sample of silica-alumina gel which exhibited an abrupt threshold diameter. In private communications with Dr. N. M. Winslow of Prado Laboratories, this phenomenon has been reported for a wide variety of materials. Apparently, a peak in the equilibrium time curve always occurs when there is an abrupt change in volume of mercury intruded. Dr. Winslow has also reported that multiple peaks are observed for samples which exhibit multiple abrupt changes in their pore size distributions.

Figure 17 shows the appearance of a fractured surface of a mature cement paste (water:cement ratio 0.4) at two stages of intrusion. For comparison, an unintruded but similar fracture surface is also illustrated. The lighter-colored and much less intruded sample was intruded to

Figure 17

Fractured Surfaces of Cement Pastes
top: Unintruded
middle: Slightly Intruded
bottom: Massively Intruded

a diameter just larger than the beginning of the peak in the equilibrium time curve. The darker sample was intruded to a diameter corresponding to the longest period of equilibrium (the top of the peak). From these samples it is apparent that the occurence of the peak corresponds to a uniform and massive intrusion of the entire sample.

It is believed that the diameter at which this massive intrusion occurs is the largest diameter which is continuous throughout the cement paste. When this diameter is reached, mercury flows from essentially the surface of the sample into this continuous network and penetrates the entire mass. Thus, it has a long way to travel upon this initial penetration. Further pressuring intrudes smaller pores. However, since the mercury has already penetrated much of the sample, the distance it must travel for further intrusion is very much less than the distance for first intrusion. Thus, the time required for mercury to flow into the finer pores is less. If the initial massive intrusion were not into a continuous pore system then the time required for future intrusion would not be so greatly reduced.

It should be noted that failure to allow the mercury to reach equilibrium will result in pore volumes being measured at erroneous diameters. If pressure is increased before equilibrium is reached, then that volume of mercury which was not allowed to intrude at the proper pressure will intrude at the higher pressure. Thus, the measured volume of smaller pores will be artificially enhanced. This danger is particularly prevalent in instruments which automatically raise the pressure.

Equilibrium of Water Vapor Sorption

As shown in Figures 13 and 14, the cement paste samples had not reached equilibrium with the water vapor even after a period of about two weeks. Feldman (8) has proposed the penetration of water molecules into inter-layer spaces in the cement hydration product. He has termed this "irreversible sorption". Eipeltauer, Schilcher and Czernin (7) have proposed a similar sort of phenomenon which they call "persorption". Indeed, it is not surprising that water vapor should be able to interact with cement paste in other than purely physical ways. Also, of course, some continued hydration of the cement may occur when it is exposed to water vapor.

It is not hard to imagine that any of these processes would be fairly slow. However, capillary condensation should be very rapid and subject only to the time required for the water vapor to diffuse to the site of a pore. Of course, for purposes of pore size measurements only capillary condensation is of interest. In this work, capillary condensation and other methods of water uptake were separated on a kinetic basis. The sharp break in the rate of water sorption curves at 24 hours was taken to be the point at which the capillary condensation had ceased. Of course, this is not an absolute break point and some other means of water uptake probably act earlier than 24 hours and some capillary condensation may occur after 24 hours. However, in view of the rapidity of the process of capillary condensation and in view of the shape of the rate curves, the selection of 24 hours does not seem unreasonable.

Commonly, when sorption has progressed as far as is desired at one partial pressure, the partial pressure is then altered without outgassing the sample. If this had been done for the cement paste used here, there

would have been a "carryover effect" due to the non-capillary condensation gain in weight. At a higher partial pressure additional capillary condensation and the long term sorption, which had not been allowed at the lower partial pressure, would both have occurred. Thus, it was necessary to outgas the sample immediately prior to each sorption step.

Also, in the normal method of adsorption, a larger pore that is accessible through a narrower neck has had its access, the narrow neck, blocked at a lower partial pressure. Thus, it is with difficulty that condensation occurs in the larger pore at the appropriate partial pressure. However, with outgassing between each step no such blocking occurred and condensation can proceed in the larger pore at the proper partial pressure.

Interpretation of Pore Size Distributions

The Powers Model

A model of the microstructure of hardened Portland cement paste has slowly evolved. As such a large part of the work on which the model is based is due to T. C. Powers, the model is often called the Powers model. A current description of this model is given by Verbeck (21). The salient portions of the model relevant to pore structure will be briefly outlined.

When Portland cement and water are mixed, large water-filled pores exist between the grains of unhydrated Portland cement. The volume and size of these large pores depends on the water:cement ratio of the mixture. The unhydrated cement and water react and yield several products, the predominant one of which is a poorly crystalline calcium silicate

hydrate which is usually called CSH gel. The specific volume of the hydration products is greater than that of the unhydrated cement. The hydration products are deposited in the large water-filled pores which exist between the unhydrated cement grains, and also in some of the space vacated by the previously unhydrated cement. During hydration the apparent bulk volume of the mix remains essentially constant. The gel which is formed has a characteristic pore volume and these pores have a characteristic size. As the gel is deposited in the large water-filled spaces it gradually isolates these spaces from their neighbors and after sufficient hydration, for normal water:cement ratios, the large pores become discontinuous. Pores with diameters between 13μ and 0.008μ are considered to have their origins primarily in the initial spaces between unhydrated grains and the diameter of the characteristic pores in the gel is considered to vary between 0.008μ and 0.001μ.

From the above it is possible to draw several conclusions about the nature and evolution of the pore structure of cement paste. Since the bulk volume of the mix is approximately constant and the specific volume of the hydration products is higher than that of the unhydrated cement then the volume of the pores must decrease as hydration proceeds. Since the hydration products are deposited in the large initial pores then the diameter and volume of the large pores must decrease. Since continued hydration produces more gel, then the volume of pores associated with the gel must increase.

Confirmation of Pore Structure Evolutionary Aspects of Powers Model

Trends in the mercury intrusion pore size distributions obtained in this work permit an appraisal of certain conclusions of the Powers model,

subject, of course, to the possible underestimation of volumes as measured by mercury intrusion. The distributions all span a pore diameter range from 210μ to 0.0085μ so the total intruded pore volume corresponds to the pore volume of the larger pores in the Powers model. From the measurement of the density of solids (made prior to initial drying) and the measurement of the bulk volume (made at the start of each porisimeter run) the total pore volume can be calculated. With the total intruded volume and the total pore volume an assessment of the volume of pores with diameters less than 0.0085μ can be made and this volume corresponds to the volume of the characteristic pores in the gel. A summation of these pore volumes for all samples tested is to be found in Table 1. The percent hydration for each sample was obtained from non-evaporable water contents using oven dried cement paste.

The data in Table 1 is in accord with the major features of the Powers model as given above. The total volume of pores is seen to decrease with increasing hydration. The volume of pores with diameters larger than 0.0085μ is seen to decrease with increasing hydration and the volume of pores with diameters less than 0.0085μ is seen to increase with increasing hydration. Finally, the total pore volume is shown to be greater for the higher water:cement ratio cement paste.

Comparison of Water Vapor and Mercury Intrusion Pore Size Distributions

The water vapor pore size distributions have been calculated down to a pore diameter of 0.0014μ. This diameter corresponds roughly to five molecular diameters. It has been mentioned that the lower limit of pore

Table 1

Summary of Pore Volume Data from Mercury Intrusion

Water:Cement Ratio	Age (days)	% Hydrated	Total Volume of Pores (ml/g)	Pores with Diameter Greater than .0085μ		Pores with Diameter Less than .0085μ	
				Volume (ml/g)	% of Total Porosity	Volume (ml/g)	% of Total Porosity
0.4	1	38.0	.323	.266	82	.057	18
0.4	2	45.7	.298	.231	77	.067	23
0.4	3	52.9	.279	.194	70	.085	30
0.4	5	59.5	.265	.182	69	.083	31
0.4	7	62.8	.260	.175	67	.085	33
0.4	28	72.4	.231	.151	65	.080	35
0.4	60	75.3	.218	.109	50	.109	50
0.4	320	80.1	.209	.100	48	.109	52
0.6	1	39.6	.412	.360	87	.052	13
0.6	2	50.2	.391	.327	84	.064	16
0.6	3	53.2	.373	.300	80	.073	20
0.6	5	61.5	.365	.272	75	.093	25
0.6	7	65.4	.360	.249	69	.111	31
0.6	28	76.5	.337	.226	67	.111	33
0.6	59	80.7	.323	.204	63	.119	37
0.6	318	86.4	.306	.187	61	.119	39

size measurement by capillary condensation is controlled by the diameter of the condensed molecules and that a pore diameter equal to about ten molecular diameters is perhaps the lower limit of the method. This may be so and the data point at 0.0014μ may be purely artificial in that the underlying assumptions of capillary condensation which were used to calculate the point are not valid. However, both distributions had ceased to register appreciable pore volumes in the fine range and it was desired to see if pushing the method to a smaller pore would indicate the presence of appreciable pore volumes in extremely fine pores. If the method is applicable at 0.0014μ then the presence of such pores is clearly indicated. In any event the portions of the distributions for larger diameters are still valid. The arithmetic summation of pore volumes by the Roberts method begins with the largest pores and works down. Thus, adding or not adding a final step or two at the small pore end in no way affects the pore volumes at larger diameters. If the distributions were terminated at a diameter of say 0.0030μ they would be identical to those presented, up to that point.

Previously, it was pointed out that the method of water vapor sorption used in this work probably allowed the water vapor to register pore volumes at correct diameters. Further, mercury intrusion was seen to be susceptible to improperly registering pore volumes due to the effect of narrow entryways. The deviations of the water vapor pore size distributions from the mercury pore size distributions are believed to arise from the improper tallying of pore volumes by mercury intrusion.

The distributions of both water:cement ratio pastes exhibit this sort of deviation in the range of diameters from 0.1000μ to 0.0400μ. It

would seem that there is a small volume of pores within this range inside the paste which are accessible only through somewhat smaller entryways. The existence of these pores as indicated by the water vapor curves does not appear to invalidate the basic idea of a threshold diameter above which few pores exist and immediately below which there exists a considerable volume of pores.

After this "large diameter" deviation of the pore distributions, the water vapor and mercury curves rejoin (at a diameter of about 0.0400μ) for pastes of both water:cement ratios. In the range of diameters from 0.0400μ to 0.0085μ, the curves of the water:cement ratio 0.6 paste exhibits truly remarkable coincidence. However, in this range the distributions of the water:cement ratio 0.4 paste again diverge and down to the finest pore measurable with mercury intrusion never again converge. The mercury intrusion clearly tallies a considerable volume of pores between the point of divergence (approximately 0.0250μ) and 0.0085μ. However, the water vapor registers more volume. The water:cement ratio 0.4 paste is a tighter, more densely packed arrangement of particles than is the 0.6 paste as a simple measurement of bulk density will show. Thus, it is reasonable that some pores in the tighter cement paste will have sufficiently narrower entryways to be unavailable to mercury even at the maximum pressure which could be achieved experimentally. It appears that the water:cement ratio 0.6 paste is open enough to permit mercury to truly measure pore volumes while the 0.4 paste is not. Presumably, at a higher pressure (smaller pore diameter) mercury would enter all the pores in the water:cement ratio 0.4 paste and the tallied volumes of the two methods would again converge.

It might be considered that, to a limited extent, the water:cement ratio 0.4 paste is discontinuous in the Powers sense. For this cement paste, mercury is reaching about half of the pore volume and the evidence cited previously is that this volume is spread throughout the paste mass in a continuous manner. However, the pore volume which is reached by water vapor but not by mercury may indeed be completely sealed off by the hydration products and, in this sense, the mature water:cement ratio 0.4 paste might be looked upon as partially discontinuous. If this is so then it is reasonable to expect this partial discontinuity to develop with age. Examination of Figures 9 and 10 shows that the pore size distributions of the 60 day and 320 day samples are of a somewhat different shape than those of the younger samples. The curves exhibit a marked flattening at finer diameters. Examination of Figures 11 and 12 does not reveal this phenomenon for the water:cement ratio 0.6 samples. Thus, one might surmise that as age advances the water:cement ratio 0.4 samples become sufficiently tight to exclude mercury from some of the pores. And further, that in view of the shapes of the distribution curves, if this exclusion occurs for any but the mature 0.4 samples, it is of much less significance.

Previously, certain aspects of the Powers model were assessed using data from mercury intrusion pore size distributions. Clearly, the assessment of these aspects is valid only in so far as the method of mercury intrusion provides a valid measure of pore size distribution. If it is true that capillary condensation of water vapor more truly measures pore sizes and volumes (because of its ability to surmount the obstacle of a narrow entryway) then the validity of the mercury intrusion

measurements would appear to be in jeopardy. It will be recalled that one fundamental quantity used in the assessment of the Powers model was the volume of pores intruded by mercury down to a diameter of 0.0085μ. Now, if this volume is erroneously measured then calculations using this volume will be in error in absolute magnitude and may even be in error with respect to the trend which is exhibited.

Considering the concurrence of the mercury and water vapor pore size distributions for the water:cement ratio 0.6 cement paste it would seem that the assessment of the Powers model for this cement paste is well founded. However, mercury appears to seriously underestimate the pore volumes down to a diameter of 0.0085μ for the water:cement ratio 0.4 cement paste. If this is so then certainly the volume of pores with diameters greater than 0.0085μ has been underestimated. It has been previously suggested that the underestimation of the mercury is due to the tight and partially discontinuous structure of the water:cement ratio 0.4 cement paste and that this partial discontinuity increases with age and noticeably alters the shape of the mercury curves somewhere between 28 and 60 days.

Thus, especially for the more mature water:cement ratio 0.4 samples, the trend of the data exhibited in Table 1 would appear to have been exaggerated by the effect. Since the water:cement ratio 0.6 samples do not seem to be subject to underestimation by mercury and since they exhibit the trend it seems unlikely that the trend for the water:cement ratio 0.4 pastes is actually reversed. So, the trends shown in Table 1 would still seem to be valid for the water:cement ratio 0.4 samples and only exaggerated in the case of the older samples.

With respect to samples of both water:cement ratios a final point should be made. It is possible that there exist pores of diameters greater than 0.1μ and which are accessible only through entryways smaller than 0.0085μ. The volume of such pores would not have been tallied by mercury because of insufficient pressure to force entry. Further, the volume of these pores would never be tallied by water vapor since their diameters lie above the practical range of capillary condensation. No assessment as to the existence of these pores is possible but it should be kept in mind that neither method of measurement used in this research would indicate their presence if they do actually exist.

Surface Areas of Cement Paste

There has been considerable discussion and experimentation on the matter of the true measurement of the surface area of hardened Portland cement paste. It was not the aim of this research to study the problem of surface area measurement but data gathered in the course of this research bears on the subject and so it is here briefly presented.

B.E.T. (1) surface areas were calculated for both cement pastes on which capillary condensation measurements were made, using the water vapor isotherms that have been presented. The area of one water molecule was assumed to be $10.6A^2$.

B.E.T. surface areas were also measured using nitrogen. This work was done with an apparatus* using helium as a carrier gas and having a pump to circulate the gas through the sample. The area of one nitrogen molecule was assumed to be $16.2A^2$.

The pore size distributions also afforded an estimate of the surface

* American Instrument Co. Sor-BET, Cat. No. 5-7300.

area of the pores which are measured. This was done by assuming that the pores were cylindrical. Then the pore size distributions were divided into small increments and the volume and average diameter of each increment were used to calculate the area of each increment. This was done for the mercury pore size distributions of the samples used for capillary condensation and was extended down to a pore diameter of 0.0085μ. It was also done for the water vapor pore size distributions and two areas were determined for each sample. One was carried to a pore diameter of 0.0027μ and one further carried to a pore diameter of 0.0014μ. Thus, five different surface areas were calculated for replicate samples of two water:cement ratios. The tabulation of these areas is to be found in Table 2. Since this data is only a by-product of this research it is presented without discussion.

Table 2

Summary of Surface Areas of Cement Paste

Water:Cement Ratio Age (days) % Hydrated	0.4 266 72.1	0.6 268 78.3
Water vapor BET Area (m^2/g)	146.8	200.6
Nitrogen BET Area (m^2/g)	7.0	13.6
Area of Cylindrical Pores Intruded by Mercury down to 0.0085μ diameter (m^2/g)	5.6	28.7
Area of Cylindrical Pores in Which Water Condensed down to 0.0027μ diameter (m^2/g)	30.2	29.3
Area of Cylindrical Pores in Which Water Condensed down to 0.0014μ diameter (m^2/g)	78.0	75.9

CONCLUSIONS

1. The methods of mercury intrusion and capillary condensation of water vapor are both applicable and useful techniques for measuring the pore size distribution of Portland cement paste. In the region of pore diameters common to both methods the agreement is excellent for the relatively open-structured 0.6 water:cement ratio paste. For the relatively tight-structured 0.4 water:cement ratio paste mercury intrusion underestimates the volume of pores of certain diameter classes.

2. The evolution of pore volumes and sizes with aging, as measured by mercury intrusion, is consistent with the currently accepted model of these evolutionary changes in that, with increasing age, total pore volume decreases, the volume of large pores decreases and the volume of small pores increases.

3. The results of mercury intrusion tests indicate that, at any stage in hydration, there is a characteristic pore diameter (threshold) larger than which a comparatively small volume of pores exists and immediately smaller than which a large volume of pores exists. This threshold diameter is about 1 μ for very young pastes and decreases during the first two-thirds of hydration to about 0.1 μ ; thereafter it decreases only slightly.

4. The measured cumulative pore size distribution of all samples continuously increases from the threshold diameter down to a diameter of at least 0.0085 μ .

5. With the exception of very young pastes, cement pastes hydrated under water have one half or more of their total pore volume in the pore diameter region between 0.1 μ and 0.0085 μ .

6. In pastes of 0.4 and 0.6 water:cement ratios at all ages, the threshold diameter is approximately the upper size limit of pores which are continuous in the past and these pores alone are sufficient to form a continuous network throughout the paste mass.

7. The technique of drying cement paste affects its pore size distribution as measured by mercury intrusion. Mercury intrusion consistently measures a greater pore volume for a more thoroughly dried paste.

8. The small amount of carbonation of bulk cement paste samples due to exposure to the laboratory atmosphere does not alter the mercury intrusion pore size distributions of the samples.

9. The factor ($4\gamma \cos\theta$) used in mercury intrusion measurements is markedly affected by the drying technique used on the cement paste. In this work the measured factor for oven dried paste is 123 μlb/in.^{2} and for "P" drying it is 179 μlb/in.^{2} Assuming a surface tension for mercury of 484 dyn/cm the contact angles are 115.9° and 129.6° respectively.

10. As the time to reach equilibrium for mercury intrusion varies widely with the diameter of the pore being intruded, considerable caution in allowing time for equilibrium is required if accurate measurements of pore size distributions are to be made on cement paste.

11. At about 24 hours there is a very sharp decrease in the rate of water vapor sorption on oven dried and ground cement paste and thereafter sorption continues very slowly. It was assumed that capillary condensation was complete in 24 hours and this appears to be justified by the agreement between the water vapor and mercury results noted earlier.

LIST OF REFERENCES

LIST OF REFERENCES

1. Brunauer, S., Emmett, P. H., Teller, E., Adsorption of Gases in Multimolecular Layers, Journal of American Chemical Society 60, 309, (1938).

2. Carlo Erba Scientific Instruments, Cement Porosity According to Hydration Time, Short Notes 3, 7, (1968).

3. Copeland, L. E., Bragg, R. H., The Hydrates of Magnesium Perchlorate, Journal of Physical Chemistry 58, 107, (1954).

4. Copeland, L. E., Hayes, J. C., The Determination of Non-evaporable Water in Hardened Portland Cement Paste, American Society for Testing and Materials Bulletin No. 194, (1953).

5. Drake, L. C., Pore-Size Distribution in Porous Materials, Journal of Industrial and Engineering Chemistry 41, 780, (1949).

6. Edel'man, L. I., Sominskii, D. S., Kopchikova, N. V., Pore Size Distribution in Cement Rocks, Kolloidnyi Zhurnal 23 (2), 228, (1961).

7. Eipeltauer, E., Schilcher, W., Czernin, W., The Problem of Pore Distribution in Cement Hydration Products, Zement-Kalk-Gips, 543, (1964).

8. Feldman, R. F., Sorption and Length-Change Scanning Isotherms of Methanol and Water on Hydrated Portland Cement, Supplementary Paper No. III-23, Fifth International Symposium on the Chemistry of Cement, Tokyo, Japan, 1968.

9. Hanna, S. J., Fracture of Hardened Cement Paste, Ph.D. Thesis, Purdue University, West Lafayette, Indiana, 1968.

10. Mikhail, R. Sh., Brunauer, S., Bodor, E. E., Investigations of a Complete Pore Structure Analysis, Journal of Colloid and Interface Science 26, 45, (1968).

11. Mikhail, R. Sh., Copeland, L. E., Brunauer, S., Pore Structures and Surface Areas of Hardened Portland Cement Pastes by Nitrogen Adsorption, Canadian Journal of Chemistry 42, 426, (1964).

12. Mikhail, R. Sh., Suzy, A. S., Adsorption of Organic Vapors in Relation to the Pore Structure of Hardened Portland Cement Pastes, Highway Research Board Special Report 90, Washington, D. C., 1966, pp. 123-134.

13. Mullen, W. G., Creep of Portland Cement Paste, Ph.D. Thesis, Purdue University, West Lafayette, Indiana, 1963.

14. Powers, T. C., The Non-evaporable Water Content of Hardened Portland Cement Paste - Its Significance for Concrete Research and Its Method of Determination, American Society for Testing and Materials Bulletin No. 158, (1949).

15. Powers, T. C., The Physical Structure and Engineering Properties of Concrete, Portland Cement Association Research Bulletin No. 90, 1958.

16. Powers, T. C., Structure and Physical Properties of Hardened Portland Cement Paste, J. Amer. Cer. Soc. 41, 1, (1958).

17. Powers, T. C., Copeland, L. E., Mann, H. M., Capillary Continuity or Discontinuity in Cement Pastes, Journal of the PCA Research and Development Laboratories 1, 38, (1959).

18. Roberts, B. F., A Procedure for Estimating Pore Volume and Area Distributions from Sorption Isotherms, Journal of Colloid and Interface Science 23, 266, (1967).

19. Thomson, W., On the Equilibrium at a Curved Surface of Liquid, Philosophical Magazine 42, 448, (1871).

20. Verbeck, G. J., Carbonation of Hydrated Portland Cement, American Society for Testing and Materials Special Technical Publication No. 205, 1958.

21. Verbeck, G. J. in Significance of Tests and Properties of Concrete and Concrete-Making Materials, STP No. 169-A, American Society for Testing and Materials, Philadepphia, Pennsylvania, 1966, pp. 211-219.

22. Washburn, E. W., Note on a Method of Determining the Distribution of Pore Sizes in a Porous Material Proceedings of the National Academy of Science 7, 115, (1921).

23. Wexler, A., Hasegawa, S., Relative Humidity-Temperature Relationships of Some Saturated Salt Solutions in the Temperature Range 0° to 50°C, Journal of Research of the National Bureau of Standards 53, 19, (1954).

APPENDIX A

APPENDIX A

Table 3

Laboratory Report of Purdue Lab Cement No. 317

DATE March 8, 1963

SAMPLE Silo # 14

Type I Lone Star Cement

TESTED BY Greencastle

CHEMICAL ANALYSIS:	
SiO_2	21.76
Al_2O_3	5.41
Fe_2O_3	1.97
CaO	65.30
MgO	1.11
SO_3	2.43
Loss	1.78
Total	99.66
Free Lime	0.72
Insol. Res.	0.27
Factor	2.41
Ratio	2.97
A/F	2.75

COMPOUND COMPOSITION:	
C_3S	51.20
C_2S	23.83
C_3A (C_2F)	11.00
C_4AF	5.99
$CaSO_4$	4.13
Na_2O	0.08
K_2O	0.46
Total Alkalies	0.38

PHYSICAL TESTS:	
Normal Consistency	25.0
Expension	.203
Gilmore: Initial	3:15
" Final	5:05
Vicat	135
# 325	95.9
Wagner	1810
Blaine	3380
% Water--Cubes	480
Flow	108
Air Entrained-%	8.5
24 Hr. Temp. °F.	70
Relative Humidity	91
False Set P.M.	96.8%

TENSILE STRENGTH: 1-3 SAND:	
1 Day	220
3 Days	330
7 "	420
28 "	510

COMPRESSIVE STRENGTH 2" CUBES:	
1 Day	1470
3 Days	2880
7 Days	4370
28 "	5680

APPENDIX B

APPENDIX B

Determination of Intrusion Factor

The basic equation of mercury intrusion is:

$$D = \frac{-4 \gamma \cos \theta}{P}$$

where: D = diameter of cylindrical pore

P = pressure required to intrude pore

γ = surface tension of intruding liquid

θ = contact angle of intruding liquid on pore wall

Thus, to reduce the pressure and volume data obtained in an experiment it is necessary to assume or know θ and γ. If these are only to be known to reduce intrusion data it is unnecessary to know their values individually. All that is necessary is to know the product $(4 \gamma \cos \theta)$. Toward this end the following work was done.

A cylinder of Portland cement paste of composition identical to those used in testing was selected. One end was carefully cut square with the axis of the cylinder. Five holes were drilled in the end, parallel to the axis, along each of eight approximately equally spaced radii. These holes were drilled with a No. 92 twist drill with a diameter of 200μ. In the center of the cylinder, again, parallel to the axis, was drilled a hole 800μ in diameter. The holes were drilled to a depth of approximately 1.35 mm. Then a disk was cut from the end whose thickness was 1.219 mm. All machining was done at the Purdue University machine shop using high

precision equipment. In this way a thin wafer of cement was obtained which had 40 nearly perfectly cylindrical holes passing completely through it.

All machine operations were conducted using a saturated solution of deionized water and $Ca(OH)_2$ as a lubricant. Thus, the nature of the cement was left unaffected by the machining.

The sample was then "P" dried. The diameter of each hole was next measured four times under a microscope. Two mutually perpendicular diameters were measured on each end of each hole. The average diameter of the "drill in" side was 197μ and of the "drill out" side 206μ. The difference was due to wobble when drilling. As the wafer was cut after drilling, no chipping on the "drill out" side was observed. Variation between mutually perpendicular diameters rarely exceeded 10μ and the holes were seen to be quite circular.

To mount the wafer for the experiment, a short pin of Teflon was passed through the larger center hole so that it extended about 5 mm from both faces, and this was cemented in place. The finished specimen is shown in Figure 18.

A special penetrometer was made for this wafer. It had a standard sample bulb but a much finer capillary stem. Graduated precision capillary tubing with an inside diameter of 500μ was used. Hence, a change in volume of .0002 ml could easily be read.

The wafer was placed in the penetrometer as shown in Figure 19. The entire assembly was then again "P" dried and immediately placed in the filling device. The filling device and entire system were evacuated to a pressure slightly higher than that at which the sample had been at

Figure 18

Drilled Cement Paste Wafer

Figure 19

Wafer Mounted in Special Penetrometer

equilibrium when drying. It was found that extensive evacuation further dried the sample.

The pore size distribution of the sample was then measured. As only the drilled holes were of interest the pressuring was carried only far enough to intrude them. Thus, a plot of pressure against intrusion was obtained for pressures between about 20mmHg and 100 mmHg. To obtain greater accuracy, pressures were measured using a cathetometer to read the heights of the manometer legs. It was found that on depressuring all of the mercury flowed out of the holes. The above process was repeated several times and replicate pore size distributions as in Figure 20 were obtained.

Then the sample was dried to equilibrium in an oven at 105°C. It was loaded into the special penetrometer and the entire assembly was again oven dried. The assembly was loaded into the filling device while still hot and allowed to cool under vacuum. Then, as in the case of "P" drying, several replicate pore size distributions were obtained as shown in Figure 21.

In the above procedure, the sample is held in a horizontal plane coinciding with the plane of the penetrometer stem. Thus, the pressure resulting in intrusion of the drilled holes is just that read on the manometer.

The pore size curves show some slope in the intrusion portion of the curve. This is to be expected as the drilled holes are not all of exactly the same size.

The factor to be used in the intrusion equation is obtained by assuming that pores with the average diameter are being intruded by a

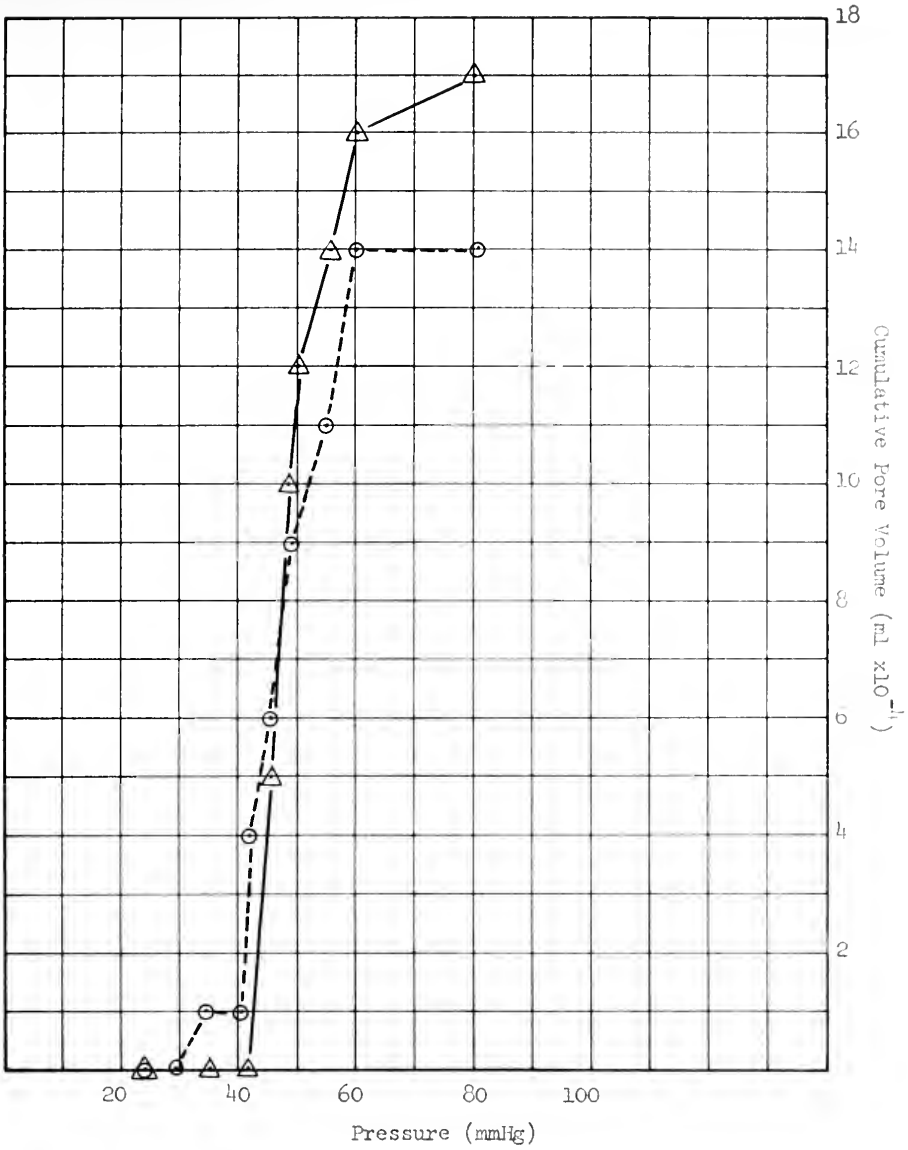

Figure 20

Pore Size Distributions
of Drilled Cement Paste Wafer ("P" dried)
Showing Duplicate Determinations

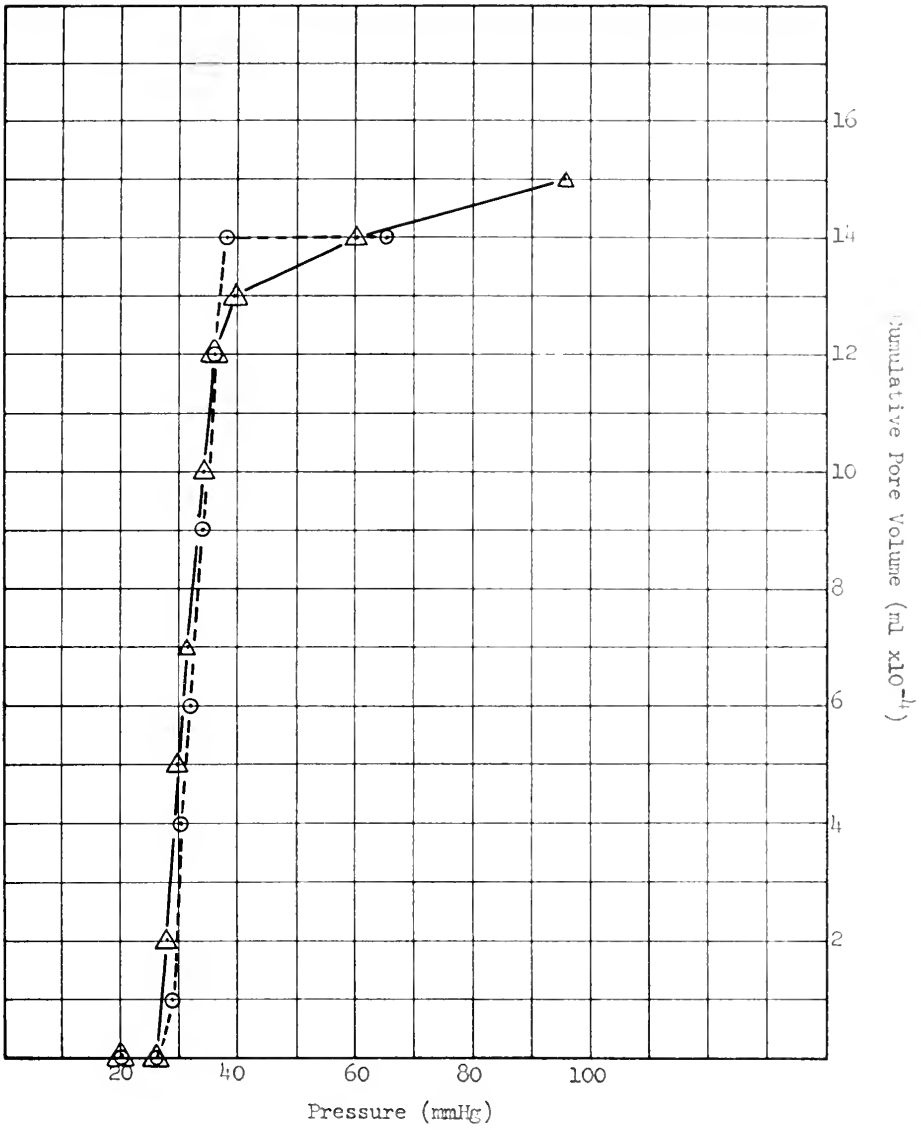

Figure 21

Pore Size Distributions
of Drilled Cement Paste Wafer (oven dried)
Showing Duplicate Determinations

pressure corresponding to one half of the total intruded volume. This system closely duplicates the actual situation when testing a sample. The pores being measured are cylindrical as are those assumed for a model when deriving the equation. The material, drying, and testing environment are exactly those which are encountered when testing. Table 4 shows the results of this work. It will be noted that if a reasonable value for the surface tension of mercury is assumed the contact angle [illegible] considerably upon drying. While this may be true, the aim and scope of this work is only the measurement of the factor for the intrusion equation.

Table 4

Summary of Intrusion Equation Factor Data

Drying Technique	Intrusion Equation Factor (μ lb in.$^{-2}$)	Contact Angle* (degrees)
'F'	17	130.5
Oven	14.3	115.9

* Assumes a surface tension of 484 dyn/cm

APPENDIX C

APPENDIX C

Measurement of t-Curve

The reduction of a sorption isotherm to a pore size distribution for a porous material requires a knowledge of the thickness of sorbed vapor on the surface of the solid. In the case of this research such knowledge was needed for water vapor sorbed onto a surface similar to that of Portland cement paste. The material selected for the determination of a t-curve must be non-porous since any capillary condensation will invalidate the results. In this case crushed quartz (Ottawa silica) was selected. Sorption measurements were made gravimetrically.

The apparatus used is shown in Figure 22 and reference will be made to the letters on the picture. The system is essentially a glass tee, A, with high vacuum stopcocks, B and C, fused to two arms. The entire system can be evacuated or vented to the atmosphere through stopcock B. The liquid controlling the partial pressure is held in a 1000 ml round bottom flask, D. This flask is joined to the system with a ground joint, E. Stopcock C is used to connect or isolate the bulb and the rest of the system. The silica is held in a sample bulb, F, which is about 120 mm in diameter. A high vacuum stopcock, G, is fused directly to the sample bulb. A small wad of glass wool is placed just below stopcock G, to prevent accidental removal of the silica from the bulb. The sample bulb is connected to the rest of the system with a short length of high vacuum rubber tubing, H.

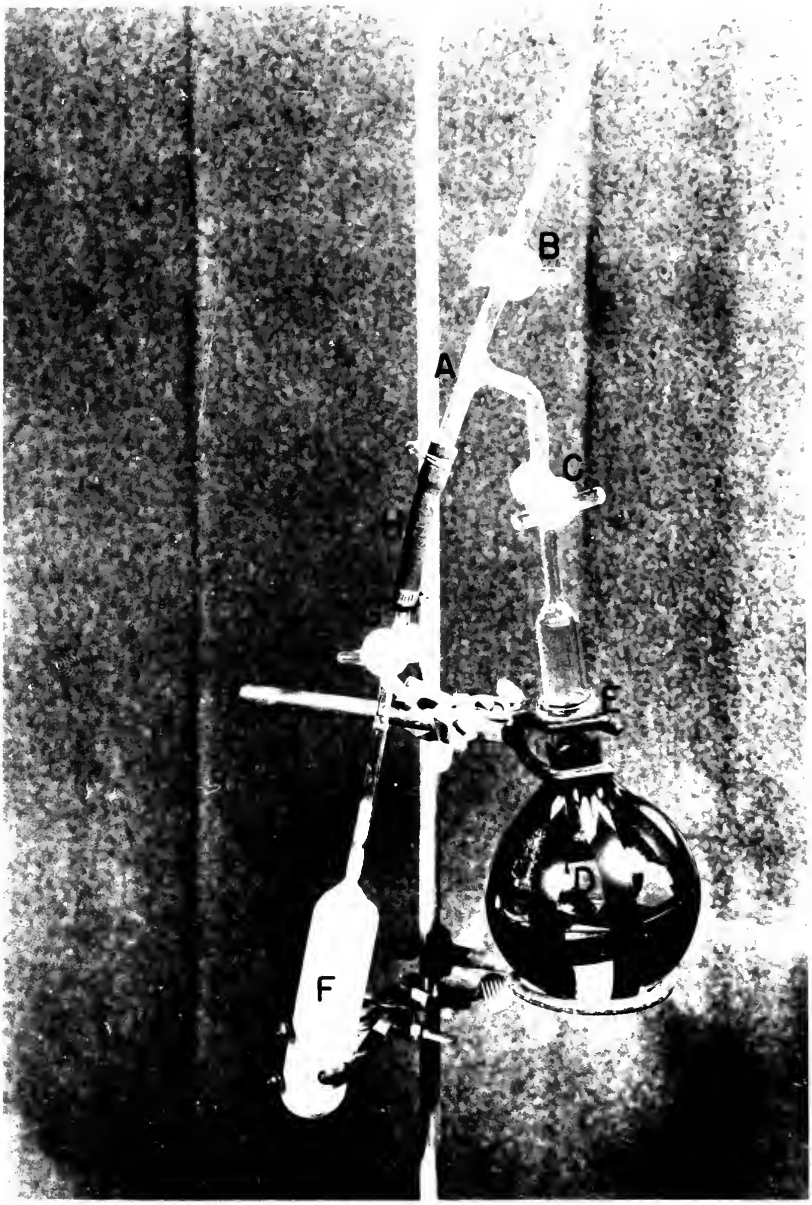

Figure 22

Apparatus for Measurement
of Water Vapor Sorption on Crushed Quartz

The silica used in the determination of the t-curve was obtained from the Ottawa Silica Company, Ottawa, Illinois. The finest portion of this powder was separated using a particle separator*. The separation produced approximately 35g of powder with a maximum diameter of five microns. This powder was sealed into the sample bulb of the sorption apparatus. The sample and bulb were then outgassed at 105°C under a continuously pumped vacuum of one micron Hg until the sample ceased losing weight. The sample was never again outgassed.

The partial pressure was controlled in the same manner as for the cement paste sorption. A solution of glycerol and water was prepared to give the desired initial partial pressure. About 500 ml of this solution was placed in the solution flask and this was attached to the sorption cell. Then the solution bulb and all tubing were evacuated to the pressure controlled by the solution. The bulb and tubing were then isolated by means of stopcock F. The sample bulb was kept isolated during this phase. The entire apparatus was placed in a constant temperature room and the sample bulb opened to the rest of the system. The solution was stirred with a magnetic stirrer.

Sorption was allowed to proceed until the sample ceased to gain weight. This was generally about two days. When the sample was to be weighed during sorption, the stopcocks G and C were closed. Then cock I was opened to the atmosphere and the sample bulb removed from the system. After weighing it was reinstalled and the tubing evacuated and closed. Then cocks C and G, were opened and sorption allowed to continue. This procedure was found to virtually eliminate any changes in the concentration of the solution due to repeated pump-down. Also, it precluded the

* American Instrument Company, Model No. 5-446.

possibility of the sample sorbing water from the air during weighing. This was found to be important.

After equilibrium was reached, a new solution was prepared and the process repeated except that the sample was not dried between steps. Sorption was measured in steps of increasing partial pressure.

Desorption measurements were made over the entire range of partial pressures after the last adsorption step was complete. This was done in the same way as adsorption except that saturated salt solutions (23) were used instead of glycerol/water solutions. The adsorption and desorption isotherms were found to exactly coincide as shown in Figure 23.

The surface area of the silica was determined from the low partial pressure region of the isotherm using the B.E.T. theory (1) . The area of a water molecule was assumed to be $10.5A^2$ and the surface area of the silica was found to be 3.10 m^2/g. The thickness of the sorbed layer at each partial pressure was then found by dividing the volume sorbed by the surface area, and the resulting t-curve is shown in Figure 24.

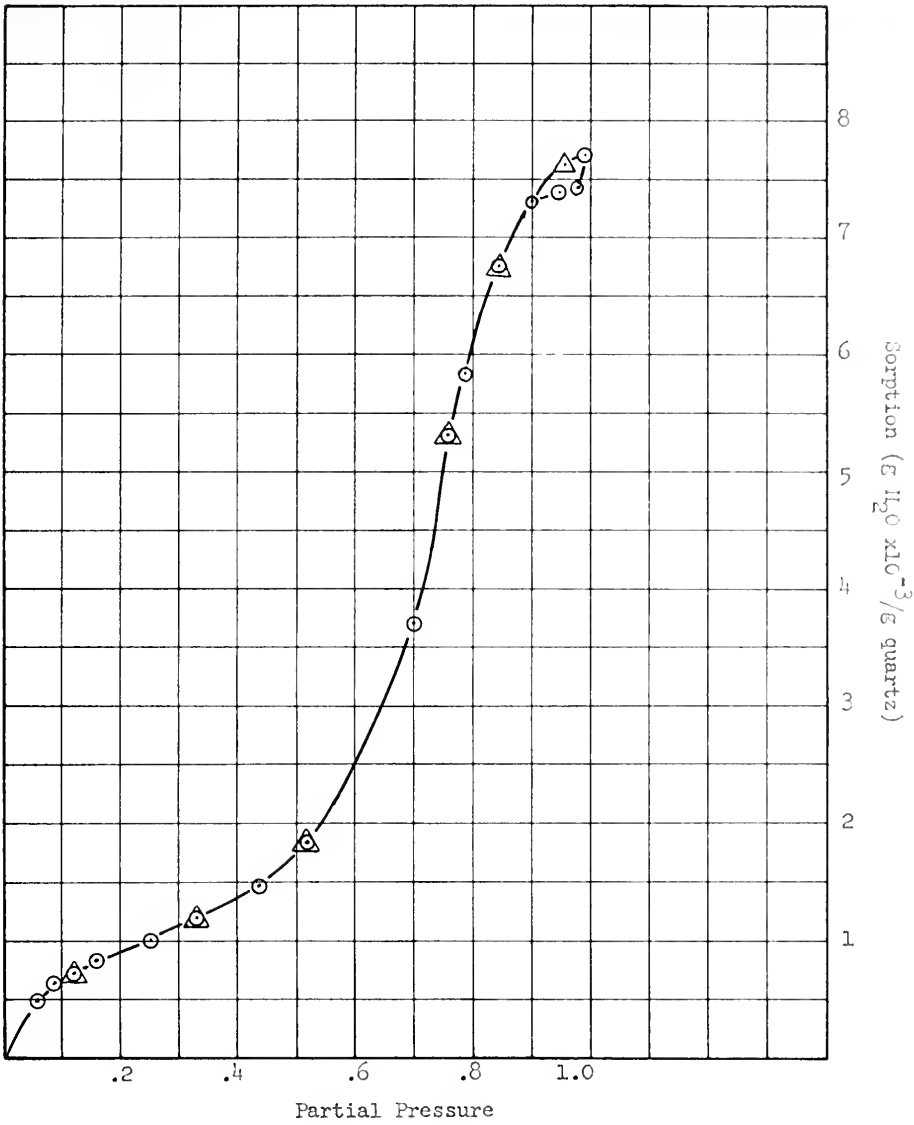

Figure 23

Water Vapor Sorption Isotherm
on Crushed Quartz at 28°C
Showing Adsorption (⊙) and Desorption (△)

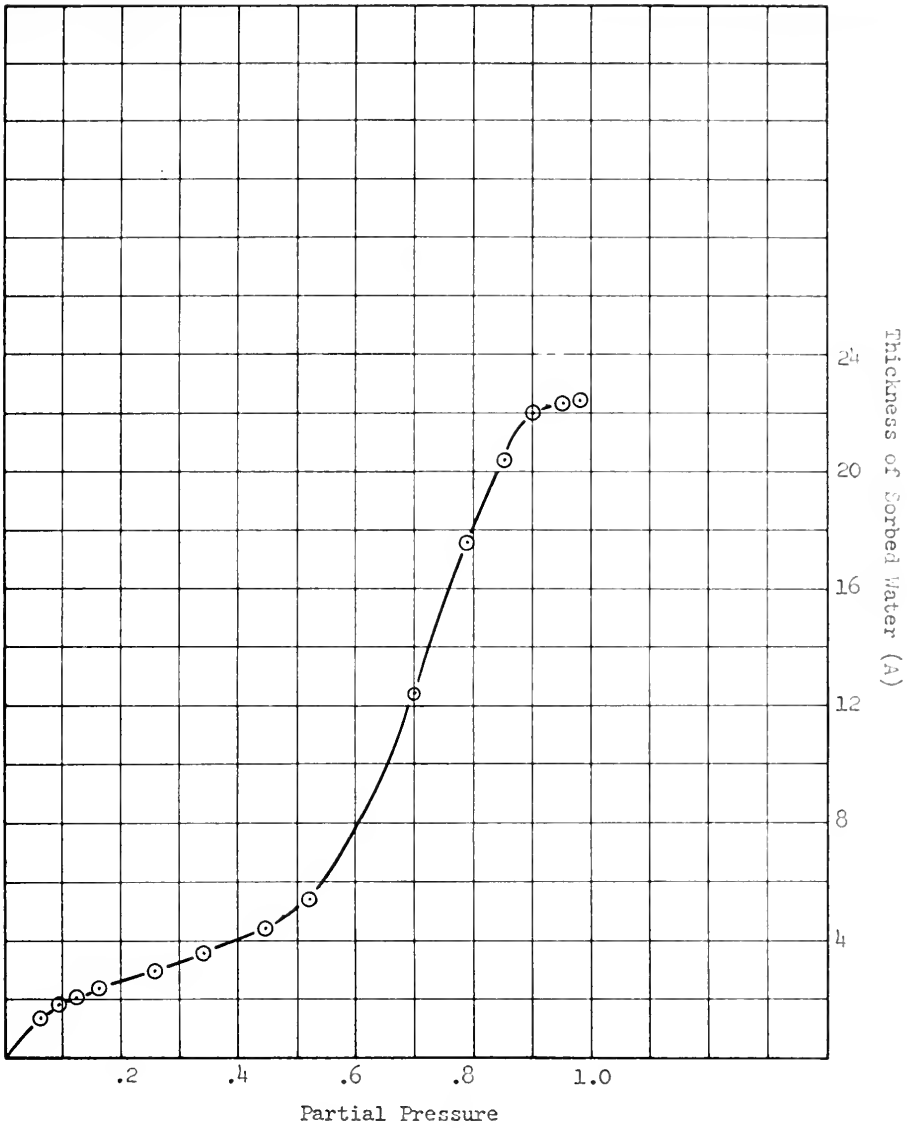

Figure 24

t-curve for Water Vapor
on Crushed Quartz at 28°C

APPENDIX D

APPENDIX D

Table 5

Basic Data for Mercury Intrusion Tests

Water: Cement	Age (days)	Test Number	Sample Weight (g)	% Hydrated	Total Pore Volume (ml/g)
0.4	1	112	.4723	38.0	.323
0.4	1	113	.4535	38.0	.323
0.4	2	114	.4672	45.7	.298
0.4	2	116	.3780	45.7	.298
0.4	3	33	.9652	52.9	.278
0.4	3	44	.6606	52.9	.278
0.4	5	115	.3945	59.5	.265
0.4	5	117	.3599	59.5	.265
0.4	7	118	.3753	62.8	.259
0.4	7	124	.3816	62.8	.259
0.4	28	133	.2545	72.4	.231
0.4	28	135	.3523	72.4	.231
0.4	60	128	.6289	75.3	.218
0.4	60	130	.6331	75.3	.218
0.4	320	66	.3450	80.1	.209
0.4	320	125	.4323	80.1	.209
0.6	1	30	.3510	39.6	.411
0.6	1	82	.4690	39.6	.411
0.6	2	99	.3974	50.2	.391
0.6	2	101	.3281	50.2	.391
0.6	3	45	.5716	53.2	.373
0.6	3	97	.5144	53.2	.373
0.6	5	100	.3855	61.5	.365
0.6	5	102	.4258	61.5	.365
0.6	7	32	.4684	65.4	.360
0.6	7	98	.5243	65.4	.360
0.6	28	103	.3432	76.5	.337
0.6	28	104	.4419	76.5	.337
0.6	59	109	.3669	80.7	.323
0.6	59	111	.4752	80.7	.323
0.6	318	106	.4720	86.4	.306
0.6	318	107	.4083	86.4	.306

Table 6

Specific Data for Each Mercury Intrusion Test

Absolute Pressure (psia)	Cumulative Intrusion (ml/g)
Test Number 30	
17	.0011
35	.0023
70	.0083
98	.0197
117	.0487
175	.1325
219	.1561
292	.1792
438	.2043
583	.2265
875	.2484
1165	.2641
1750	.2806
2190	.2940
2920	.3100
4380	.3265
8750	.3464
10000	.3493
15000	.3575
Test Number 32	
17	.0004
117	.0017
250	.0032
350	.0043
438	.0058
583	.0162
875	.0625
1165	.0969
1750	.1420
1940	.1505
2500	.1674
3500	.1849
5830	.2075
8750	.2267
10000	.2331
15000	.2494
Test Number 33	
25	.0006
98	.0013
194	.0028
250	.0038
292	.0047
350	.0059
438	.0071
583	.0129
875	.0356
1165	.0680
1750	.1047
1940	.1154
2500	.1315
2920	.1413
3500	.1490
4380	.1581
5830	.1686
8750	.1806
10000	.1843
15000	.1941
Test Number 44	
250	.0008
438	.0054
583	.0141
700	.0280
875	.0430
1000	.0599
1167	.0687
1400	.0905
1750	.1102
1940	.1196
2190	.1267
2920	.1468
4380	.1645
8750	.1860
15000	.1944
Test Number 45	
117	.0017
175	.0040
194	.0108
219	.0346
250	.0660
350	.1037
438	.1184
875	.1499
1750	.2014
2500	.2302
3500	.2481
7000	.2783
10000	.2906
15000	.3009
Test Number 66	
26	.0014
251	.0029
1000	.0041
1750	.0107
2050	.0241
2500	.0406
3200	.0525
4400	.0632
5800	.0713
8600	.0843
10000	.0901
15000	.0994

Table 6 (cont'd.)

Absolute Pressure (psia)	Cumulative Intrusion (ml/g)
Test Number 82	
26	.0158
111	.0571
251	.1832
581	.2298
1000	.2571
1700	.2853
2200	.3004
2700	.3126
3900	.3286
5800	.3409
8600	.3514
15000	.3648
Test Number 97	
176	.0276
221	.0486
291	.0842
581	.1252
1000	.1697
1400	.1995
2000	.2288
5000	.2683
15000	.3056
Test Number 98	
291	.0040
701	.0278
1000	.0799
1400	.1221
2050	.1497
3900	.1909
7000	.2176
15000	.2489
Test Number 99	
96	.0081
176	.0297
251	.1127
436	.1595
1000	.2058
1800	.2519
2900	.2813
5000	.3027
10000	.3251
Test Number 100	
176	.0039
351	.0161
701	.0918
1200	.1437
2000	.1842
2900	.2054
5800	.2420
15000	.2719
Test Number 101	
111	.0076
196	.0637
351	.1378
581	.1646
876	.1887
1400	.2295
2300	.2673
3900	.2880
7000	.3069
15000	.3270
Test Number 102	
221	.0059
291	.0085
436	.0279
1000	.1252
1700	.1721
1900	.1798
2300	.1909
4400	.2278
8600	.2560
Test Number 103	
351	.0003
1150	.0216
1750	.0740
2700	.1139
4400	.1477
7000	.1795
15000	.2279
Test Number 104	
581	.0075
1000	.0118
1400	.0414
2200	.0969
3500	.1346
5800	.1681
10000	.2068
Test Number 106	
1000	.0142
1700	.0409
1900	.0494
2200	.0644
2900	.0860
4400	.1102
7000	.1390
15000	.1880
Test Number 107	
351	.0130
1200	.0176
2000	.0563
2500	.0757
3500	.1029
5800	.1296
10000	.1700

Table 6 (cont'd.)

Absolute Pressure (psia)	Cumulative Intrusion (ml/g)
Test Number 109	
351	.0071
876	.0076
1400	.0300
3500	.1218
7000	.1624
15000	.2031
Test Number 111	
1000	.0099
1700	.0642
1900	.0768
2300	.0930
2700	.1050
3200	.1162
3900	.1296
5000	.1427
8600	.1757
Test Number 112	
16	.0036
36	.0047
111	.0074
221	.0521
351	.1052
701	.1397
1200	.1658
1800	.1903
2200	.2030
2900	.2177
4400	.2346
7000	.2456
15000	.2607

Absolute Pressure (psia)	Cumulative Intrusion (ml/g)
Test Number 113	
71	.0071
176	.0203
196	.0395
291	.0977
436	.1244
581	.1387
1000	.1634
1400	.1826
3500	.2340
10000	.2635
Test Number 114	
16	.0034
36	.0043
111	.0051
196	.0066
251	.0083
436	.0715
701	.0970
1200	.1291
1700	.1539
2700	.1824
4400	.2016
7000	.2151
15000	.2330
Test Number 115	
36	.0008
221	.0025
581	.0031
876	.0035
1200	.0248
1700	.0778
2500	.1037
5000	.1452
8600	.1653
15000	.1797

Absolute Pressure (psia)	Cumulative Intrusion (ml/g)
Test Number 116	
56	.0040
291	.0087
351	.0418
581	.0849
876	.1042
1400	.1362
2200	.1672
3500	.1897
5800	.2058
10000	.2190
Test Number 117	
351	.0056
1000	.0078
1400	.0533
2000	.0942
3500	.1325
7000	.1617
10000	.1748
Test Number 118	
351	.0040
1000	.0059
1400	.0336
2300	.0933
3900	.1247
7000	.1505
11800	.1697
Test Number 124	
351	.0026
1200	.0060
1700	.0550
2000	.0755
2900	.1035
5000	.1305
8600	.1533
15000	.1731

Table 6 (cont'd.)

Absolute Pressure (psia)	Cumulative Intrusion (ml/g)
Test Number 125	
1000	.0081
1900	.0185
2500	.0396
3500	.0585
5800	.0743
15000	.1027
Test Number 128	
176	.0105
1200	.0114
1700	.0197
2200	.0456
2900	.0622
4400	.0762
7000	.0873
10000	.0972
15000	.1050
Test Number 130	
176	.0039
1400	.0058
1900	.0270
2500	.0513
3500	.0673
5800	.0820
8600	.0943
Test Number 133	
1200	.0118
1700	.0346
2000	.0507
3500	.0880
5800	.1120
10000	.1348

Absolute Pressure (psia)	Cumulative Intrusion (ml/g)
Test Number 135	
1000	.0071
1400	.0136
1800	.0369
2200	.0588
2900	.0792
4400	.0991
7000	.1212
15000	.1517

APPENDIX E

APPENDIX E

Selected Intrusion Curves

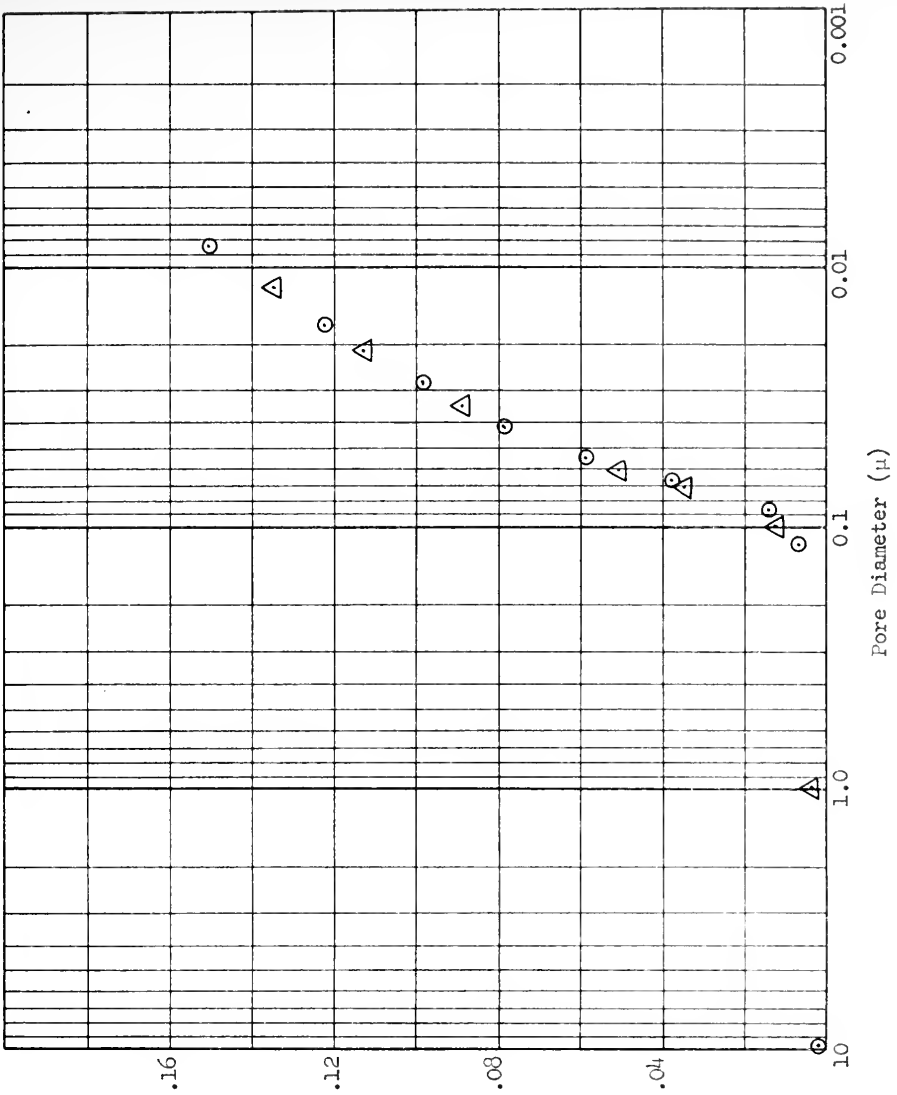

Figure 25

Pore Size Distributions
of Replicate Samples of Cement Paste
(water:cement ratio 0.4, age 28 days)

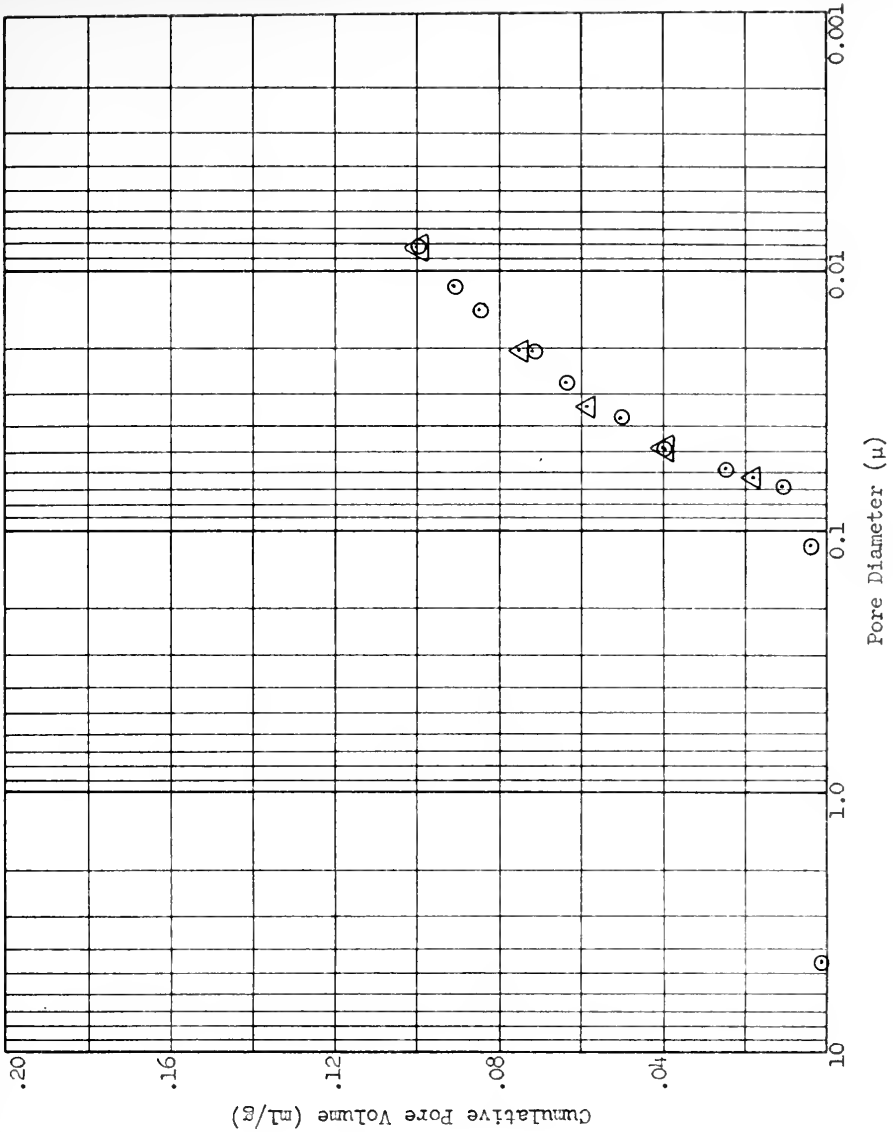

Figure 26

Pore Size Distributions
of Replicate Samples of Cement Paste
(water:cement ratio 0.4, age 320 days)

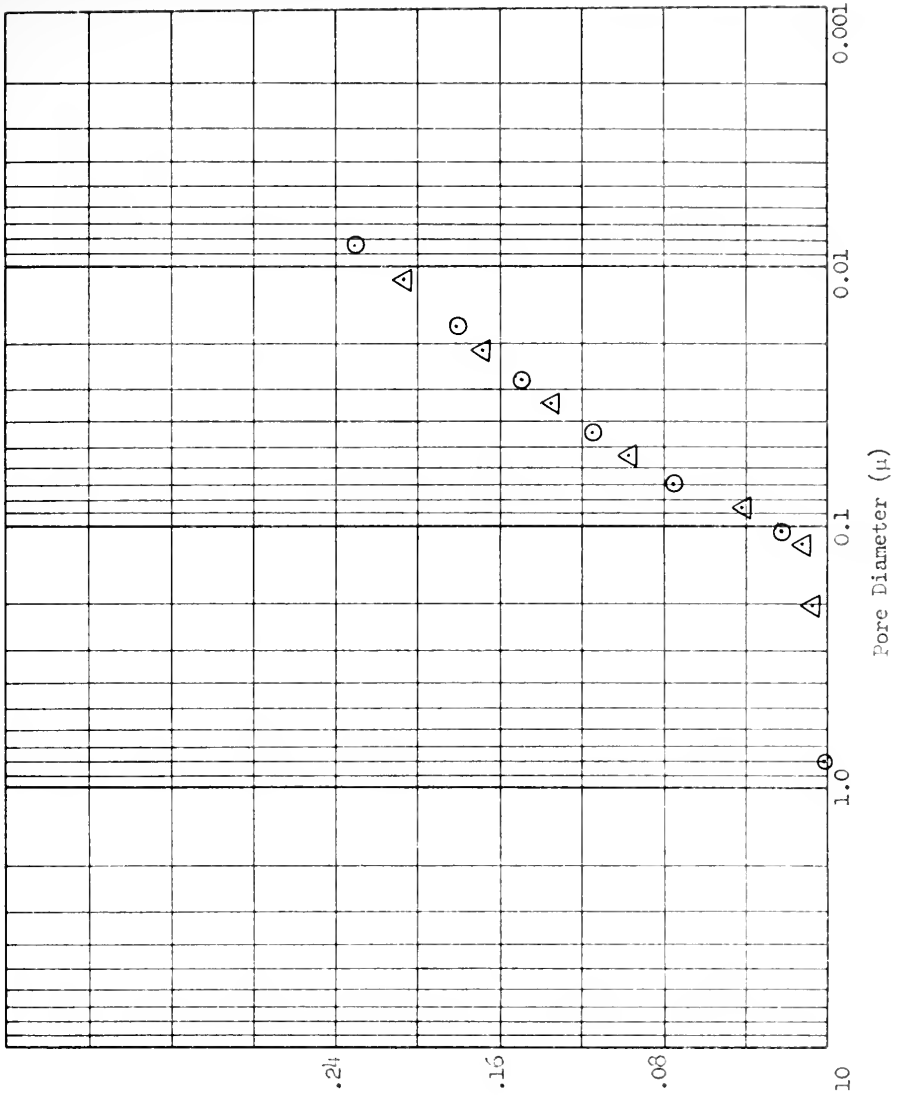

Figure 27

Pore Size Distributions
of Replicate Samples of Cement Paste
(water:cement ratio 0.6, age 28 days)

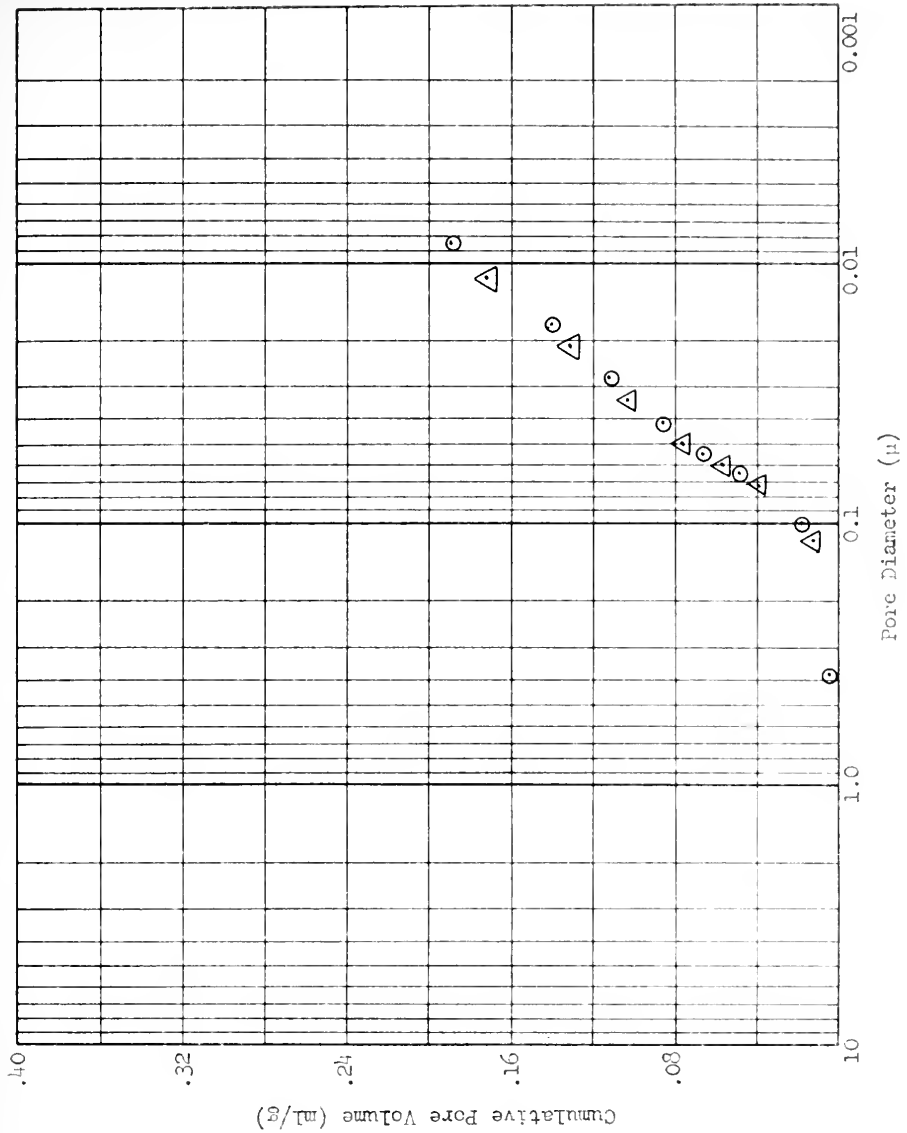

Figure 28

Pore Size Distributions
of Replicate Samples of Cement Paste
(water:cement ratio 0.6, age 318 days)

APPENDIX F

APPENDIX F

Scanning Electron Micrographs of Cement Pastes

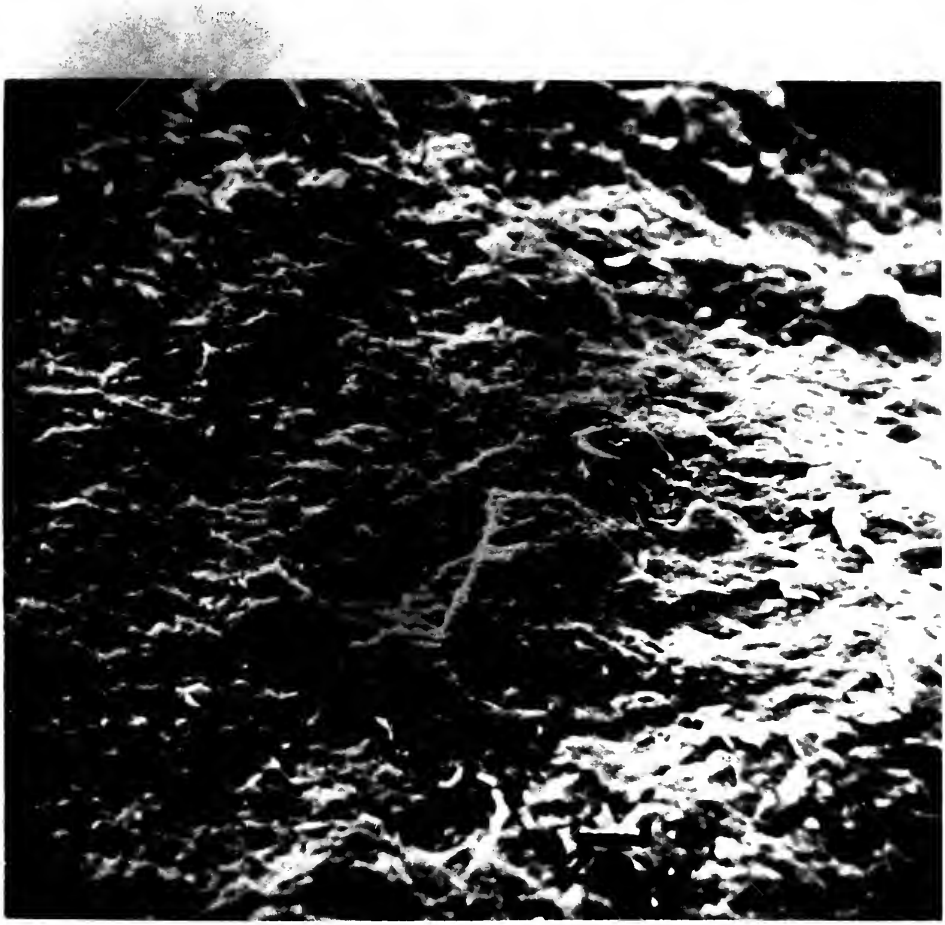

Figure 29

Fractured Surface of Cement Paste
Water:Cement Ratio : 0.4
Age: 266 days
Magnification: 340X

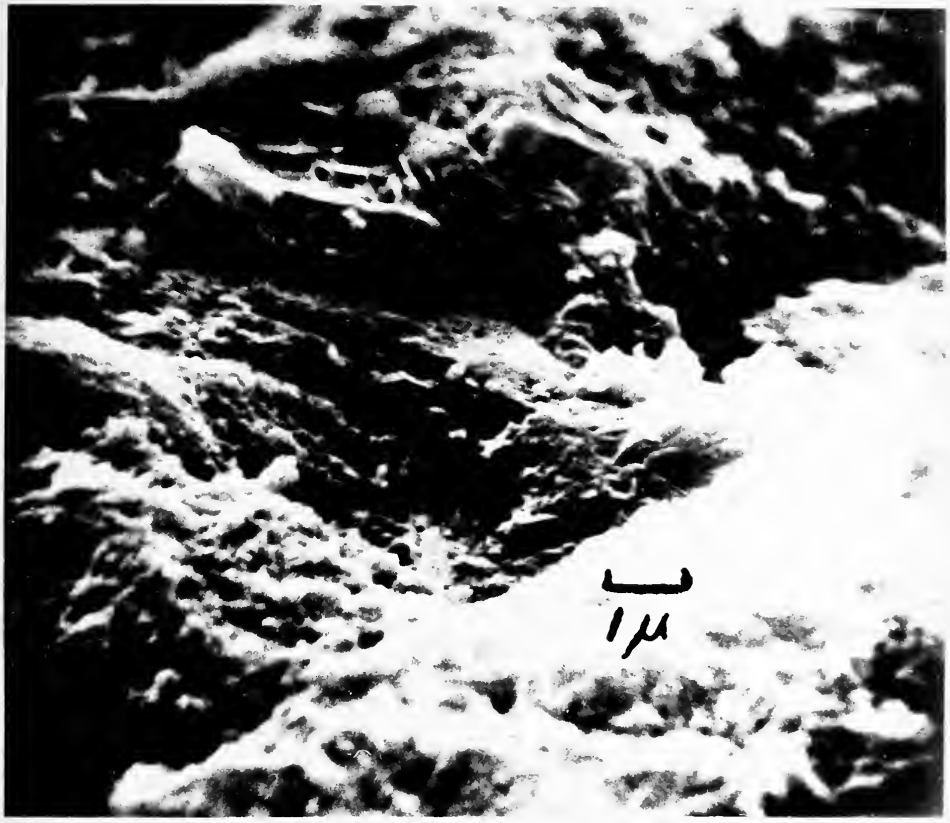

Figure 30

Fractured Surface of Cement Paste
Water:Cement Ratio: 0.4
Age: 28 days
Magnification: 50X

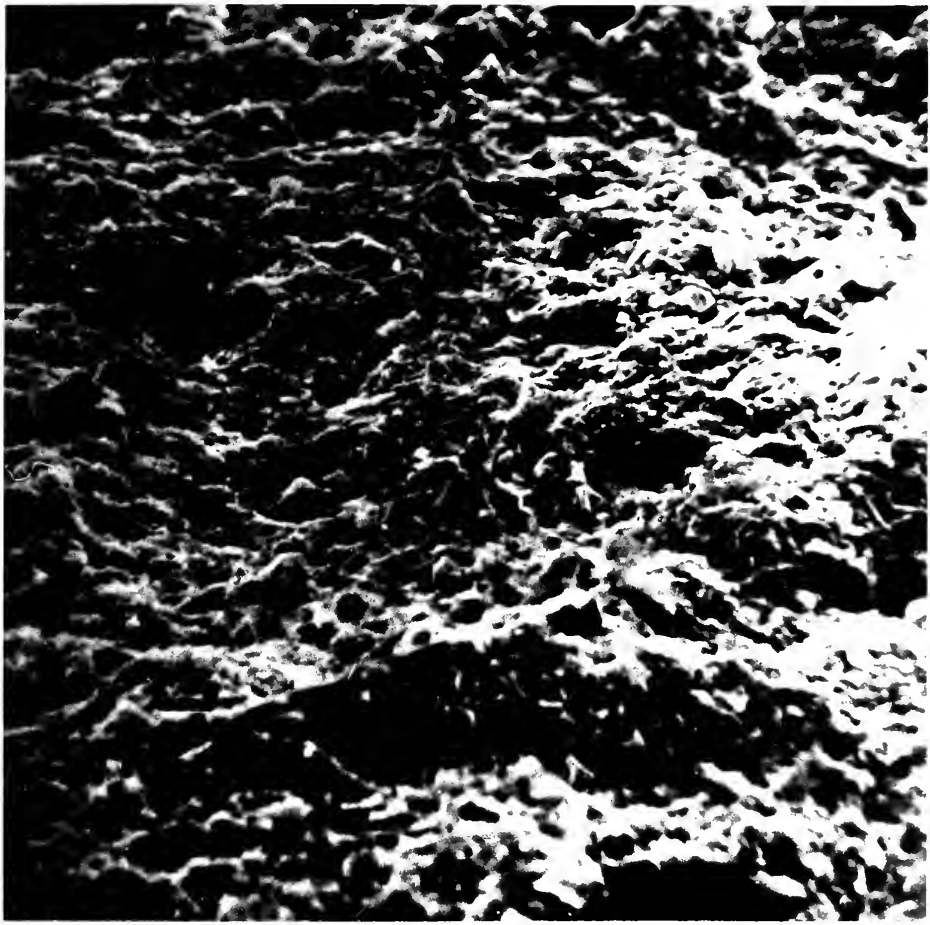

Figure 31

Fractured Surface of Cement Paste
Water:Cement Ratio: 0.6
Age: 268 days
Magnification: 260X

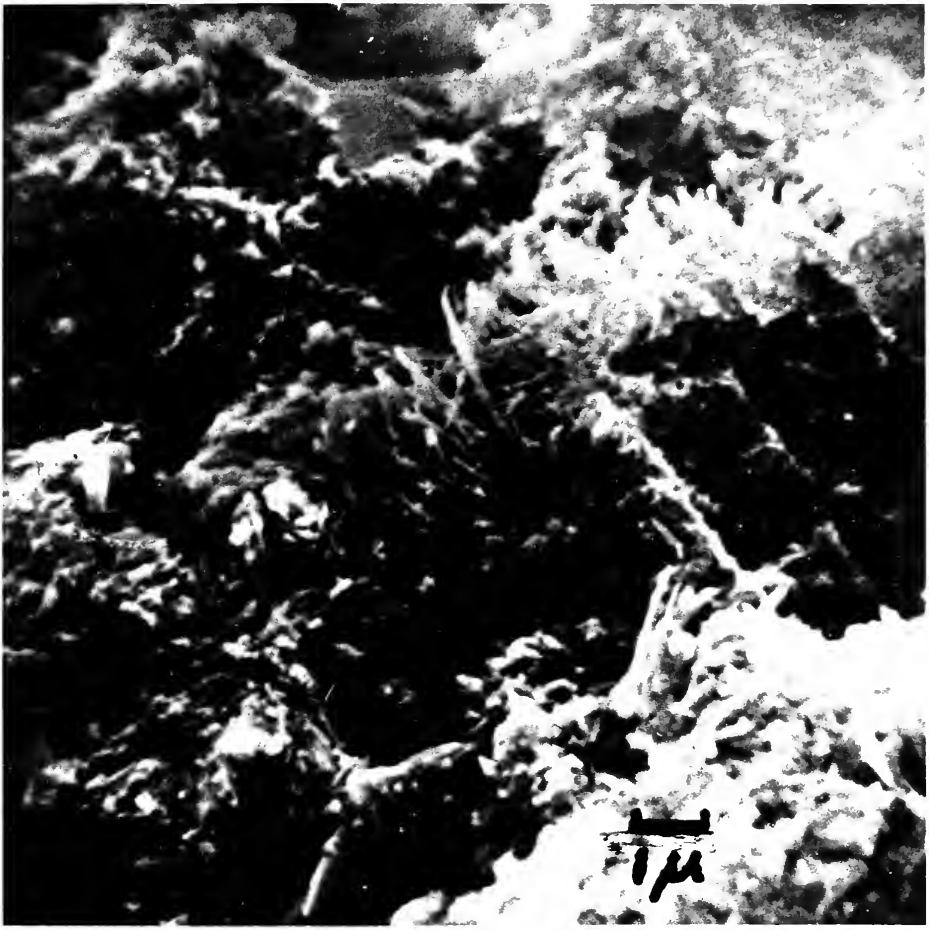

Figure 32

Fractured Surface of Cement Paste
Water:Cement Ratio: 0.6
Age: 268 days
Magnification: 6500X

APPENDIX G

APPENDIX G

Table 7

Mercury Intrusion and Capillary Condensation Data
for 0.4 Water:Cement Ratio Cement Paste (age = 267 days)

Mercury Intrusion Measurements				Capillary Condensation Measurements	
Pore Diameter (μ)	Cumulative Pore Volume (ml/g)	Pore Diameter (μ)	Cumulative Pore Volume (ml/g)	Pore Diameter (μ)	Cumulative Pore Volume (ml/g)
0.800	.0013	1.020	.0046	.1045	0.0000
.087	.0074	.102	.0068	.0945	.0097
.049	.0197	.063	.0077	.0845	.0125
.042	.0303	.056	.0109	.0745	.0164
.038	.0369	.049	.0132	.0645	.0221
.031	.0475	.042	.0295	.0545	.0279
.024	.0571	.031	.0463	.0444	.0357
.017	.0655	.024	.0564	.0344	.0452
.014	.0694	.017	.0644	.0244	.0625
.008	.0787	.008	.0773	.0219	.0693
				.0193	.0777
				.0166	.0878
				.0138	.1013
				.0114	.1120
				.0088	.1203
				.0058	.1260
				.0027	.1332
				.0014	.1581

Table 8

Mercury Intrusion and Capillary Condensation Data
for 0.6 Water:Cement Ratio Cement Paste (age = 267 days)

Mercury Intrusion Measurements				Capillary Condensation Measurements	
Pore Diameter (μ)	Cumulative Pore Volume (ml/g)	Pore Diameter (μ)	Cumulative Pore Volume (ml/g)	Pore Diameter (μ)	Cumulative Pore Volume (ml/g)
9.800	.0105	1.020	.0152	.1045	0.0000
.140	.0189	.070	.0301	.0945	.0379
.088	.0215	.061	.0387	.0845	.0418
.045	.0804	.051	.0582	.0745	.0480
.035	.1029	.020	.1420	.0645	.0560
.025	.1264	.016	.1643	.0545	.0665
.014	.1568			.0444	.0816
.008	.1938			.0344	.1000
				.0244	.1249
				.0219	.1333
				.0193	.1428
				.0166	.1543
				.0138	.1706
				.0114	.1838
				.0088	.1929
				.0058	.1980
				.0027	.1983
				.0014	.2231